Micromechanics of granular materials: slow flows

Niels P. Kruyt

Department of Mechanical Engineering,
University of Twente,

n.p.kruyt@utwente.nl
www.ts.ctw.utwente.nl/kruyt/

Applications of granular materials

- geotechnical engineering
- geophysical flows
- bulk solids engineering
- chemical process engineering
- mining
- gas and oil production
- food-processing industry
- agriculture
- pharmaceutical industry

Features

- rate-independent
- elasticity
- plasticity
- frictional
- dilatancy
- anisotropy

- viscous
- multi-phase
- cohesion
- segregation

Overview talk

- Introduction
- Continuum modelling
- Micromechanical modelling
  - Effect of interparticle friction on macroscopic behaviour
  - Validity of mean-field approaches
- Mixing in rotating cylinders

Slow granular flows

- Rate-independent; quasi-static
- Continuum level
  - stress tensor
  - strain tensor

Stress and strain tensors

- Stress tensor

$$df_i = n_j \sigma_{ji} dA$$

- Strain tensor

$$du_i = \varepsilon_{ij} dx_j$$

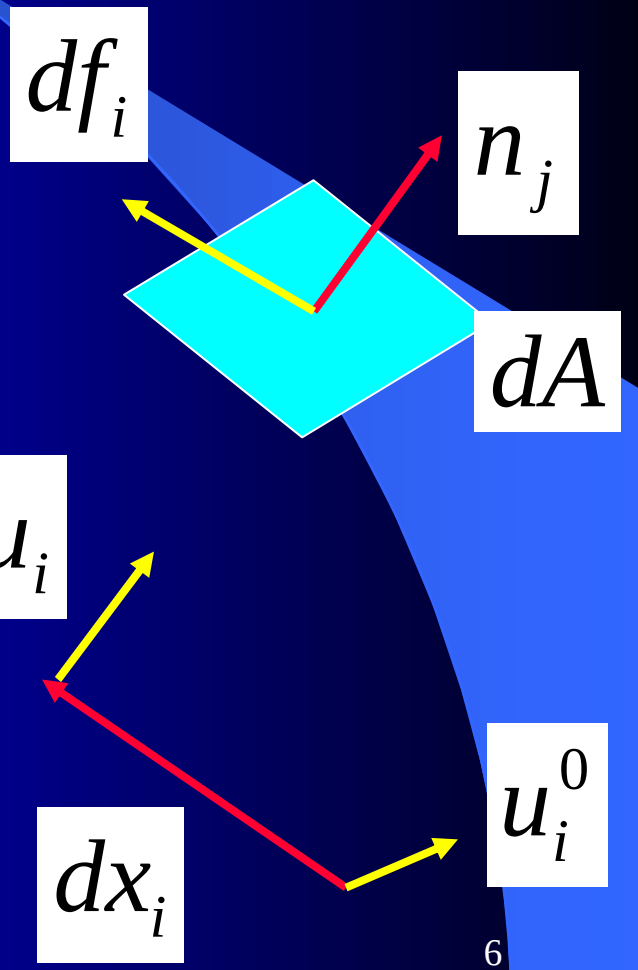

Constitutive relations

- Continuum theories; elasto-plasticity
  - elastic and plastic strains
  - yield function
  - flow rule: plastic potential
- Micromechanical theories
  - relation with microstructure

Plasticity of metals $\leftrightarrow$ granular materials

- pressure dependence
- volume changes: dilatancy
- non-associated flowrule
- strain-softening

Micromechanics of slow flows

Study relation between micro and macro level

Work with Leo Rothenburg, University of Waterloo, Canada

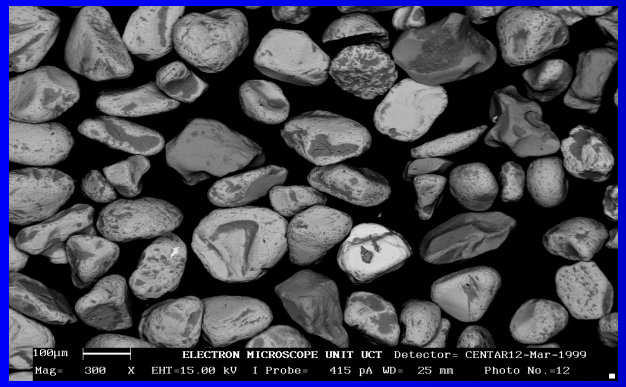

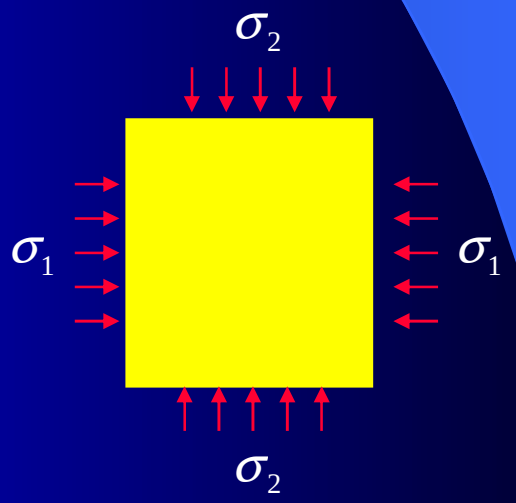

Objective

- Micro-level $\rightarrow$ macro-level
- Account for the discrete nature
- Emphasis on slow flows
  - Elasticity
  - Plasticity
- Theory and DEM simulations

From discrete information → stress and strain

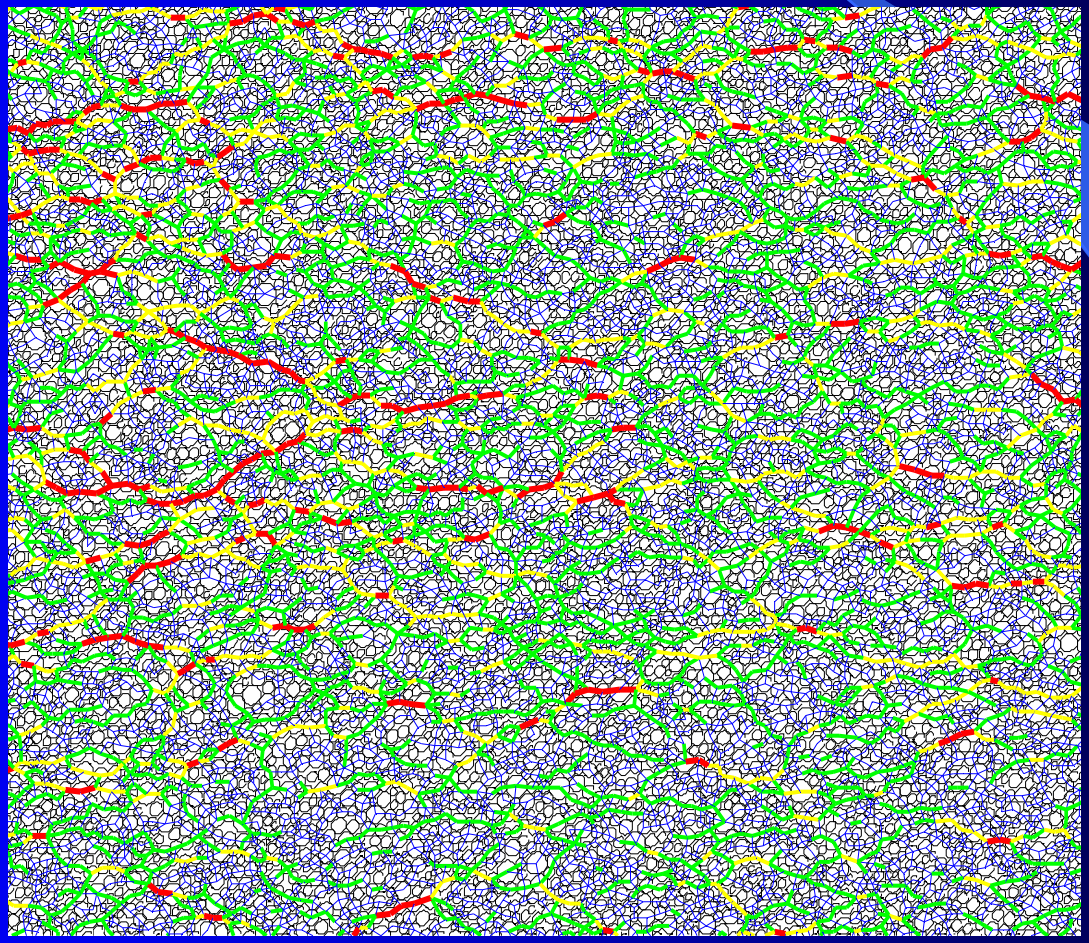

Averaging/homogenisation

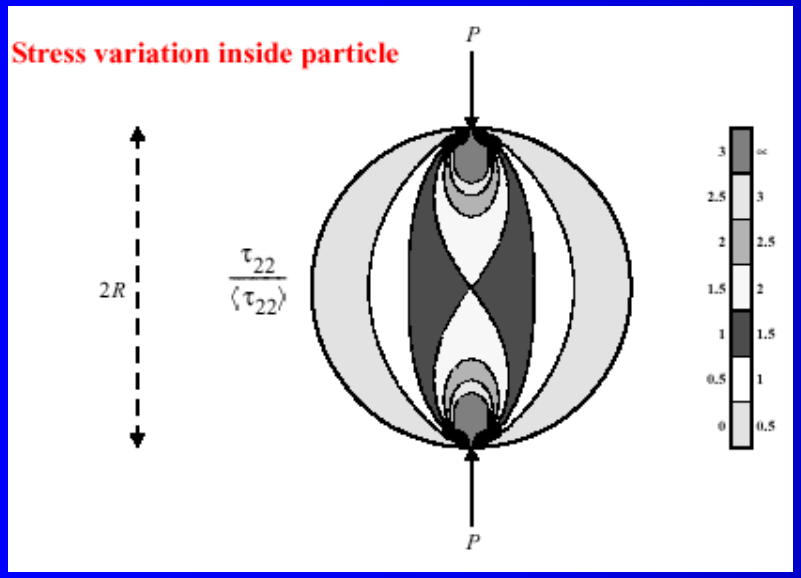

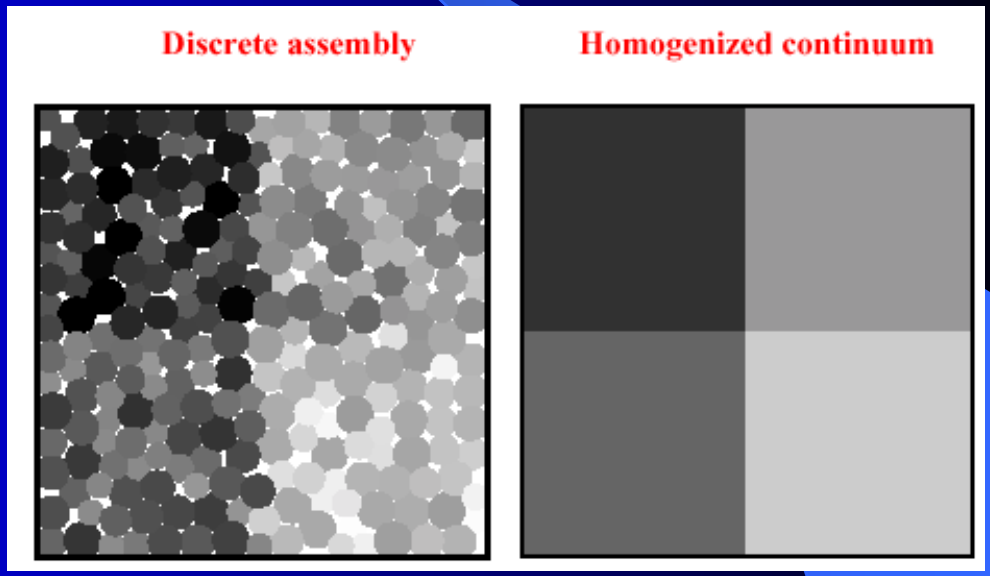

Stress

$$F_i^R = A_{\text{plane}} N_j \sigma_{ji}$$

$$\bar{\sigma}_{ij} = \frac{1}{V} \sum_{c \in C} l_i^c f_j^c$$

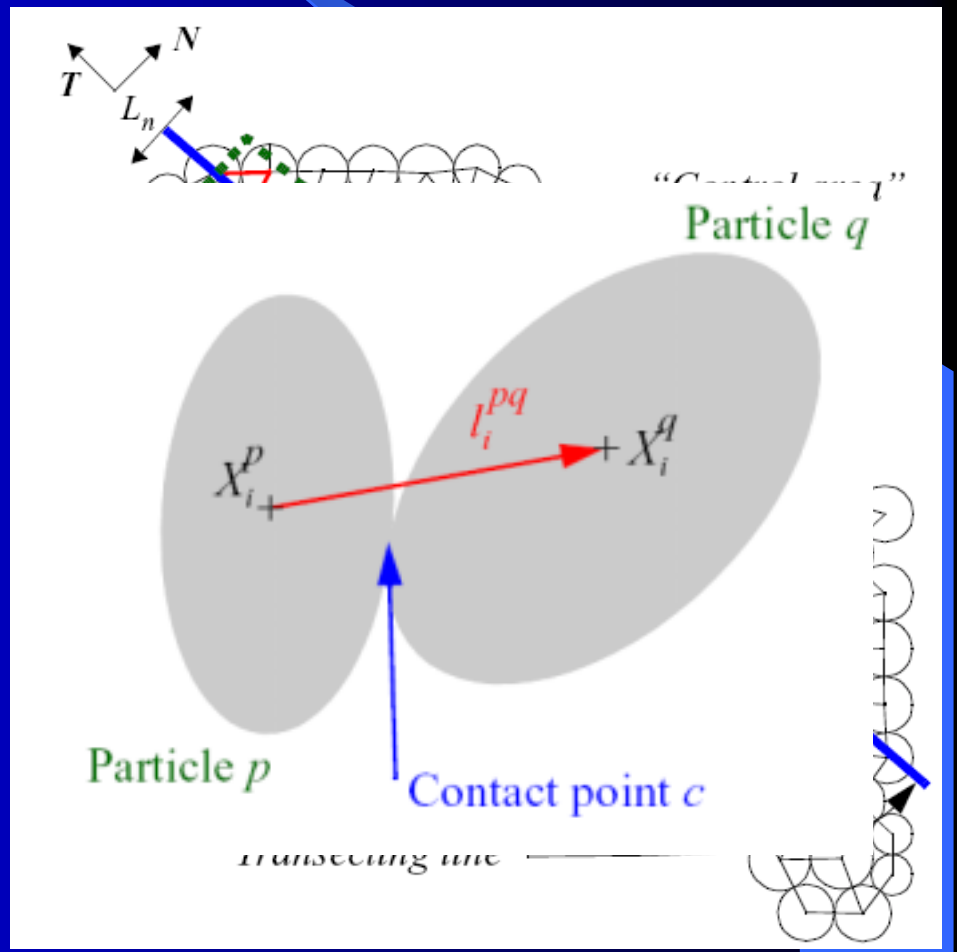

Compatibility equations

$$\Delta_i^{pq} = U_i^q - U_i^p$$

$$\sum_S \Delta_i^{RS} + \Delta_i^{R\alpha} = 0$$

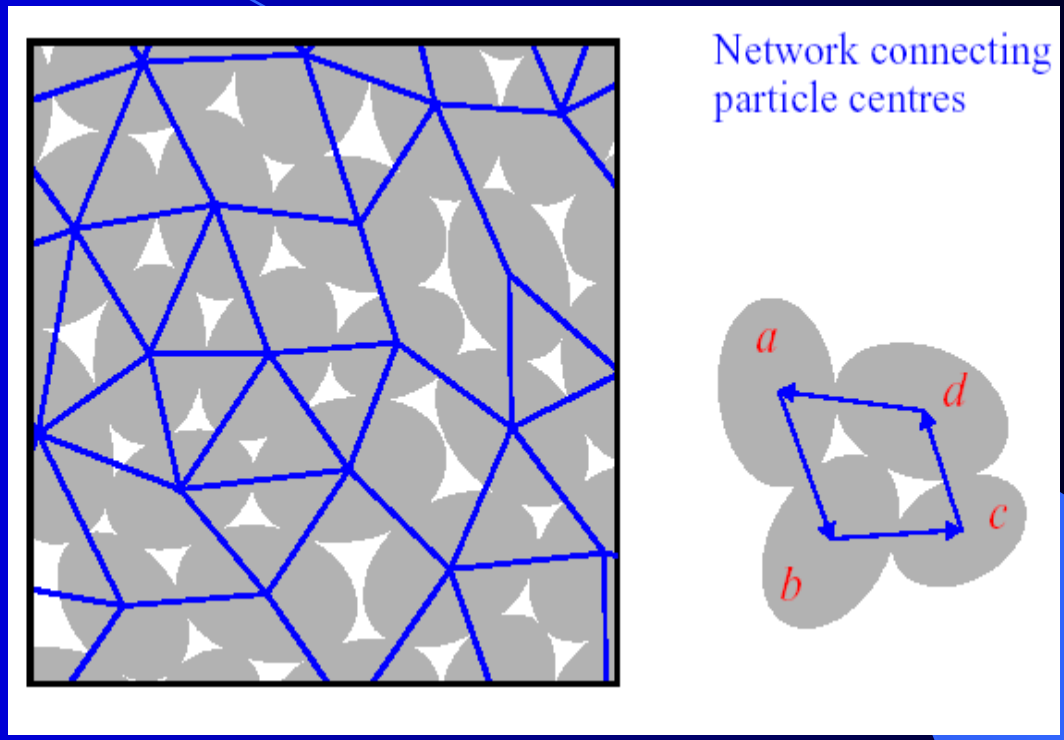

$$\sum_S \Delta_i^{RS} = \Delta_i^{ab} + \Delta_i^{bc} + \Delta_i^{cd} + \Delta_i^{da}$$
$$= \left[U_i^a - U_i^b\right] + \left[U_i^b - U_i^c\right] + \left[U_i^c - U_i^d\right] + \left[U_i^d - U_i^a\right]$$
$$= 0$$

Strain

$$dU_i^L = \varepsilon_{ij} dX_j$$

$$\bar{\varepsilon}_{ij} = \frac{1}{A} \sum_{c \in C} h_j^c \Delta_i^c$$

$$\Delta_i^{pq} = U_i^q - U_i^p$$

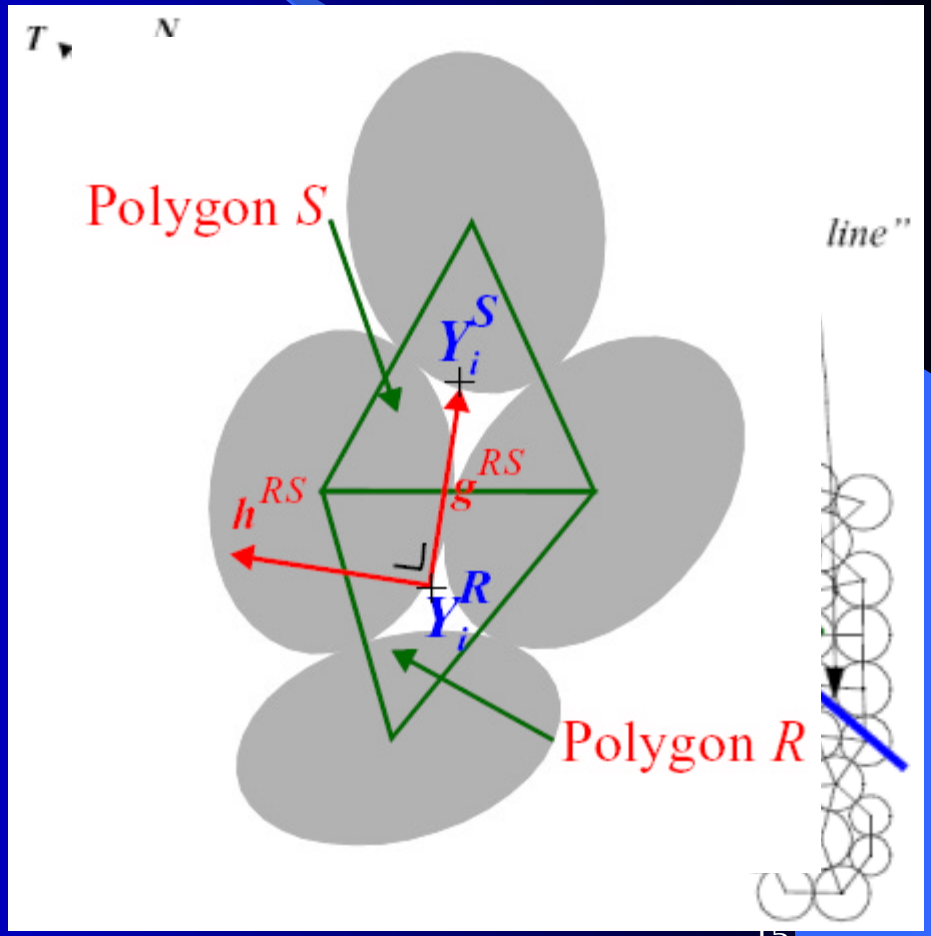

Micromechanics

Statics **Kinematics**

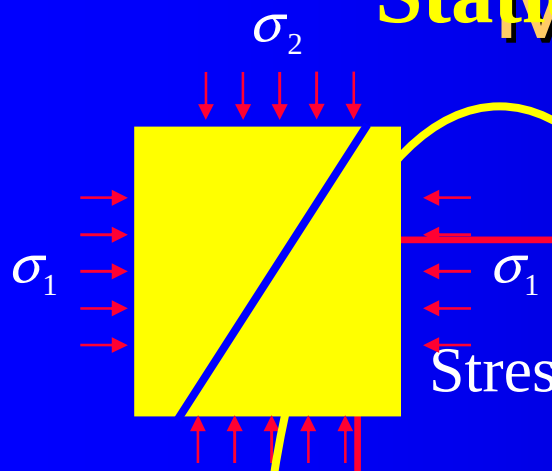

Macroscopic level (continuum)

Stress

Strain

Averaging

Localisation

Constitutive relation

Localisation

Averaging

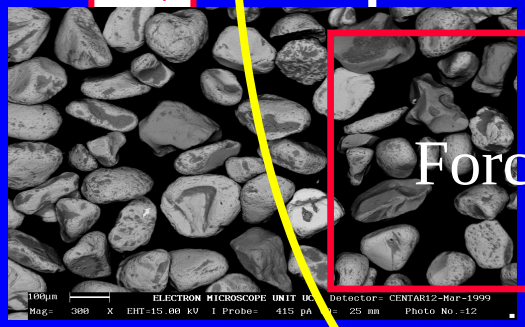

Force

Relative displace-ment

Microscopic level (contact)

Topics in micromechanics

- Importance of geometrical anisotropy
- Effect of interparticle friction on macroscopic behaviour
- Validity of mean-field approach

DEM simulations

- biaxial deformation
- two-dimensional
- **various friction coefficients μ**
- dense and loose initial assembly
- periodic boundary conditions
- 50,000 disks

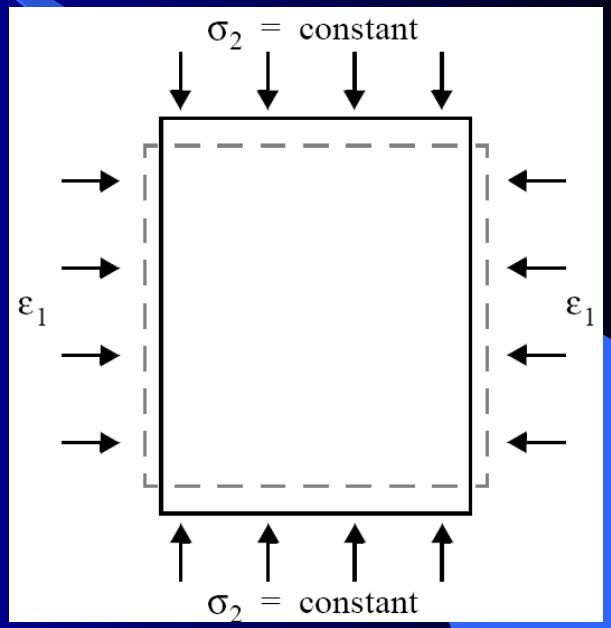

Invariants:

$$p = \frac{1}{2}(\sigma_1 + \sigma_2) \qquad \varepsilon_V = \varepsilon_1 + \varepsilon_2$$

$$q = \frac{1}{2}(\sigma_1 - \sigma_2) \qquad \varepsilon_S = \varepsilon_1 - \varepsilon_2$$

Contact constitutive relation

$$f_n^c = k_n \Delta_n^c \qquad f_t^c = k_t \Delta_t^c \qquad \left| f_t^c \right| \le \mu \cdot f_n^c$$

Special cases:

- $\mu \to 0$
- $\mu \to \infty$

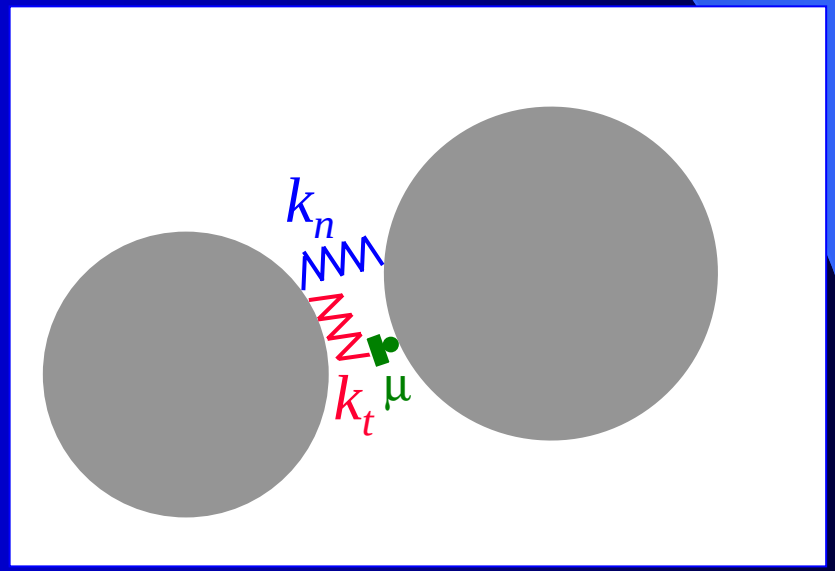

Animation

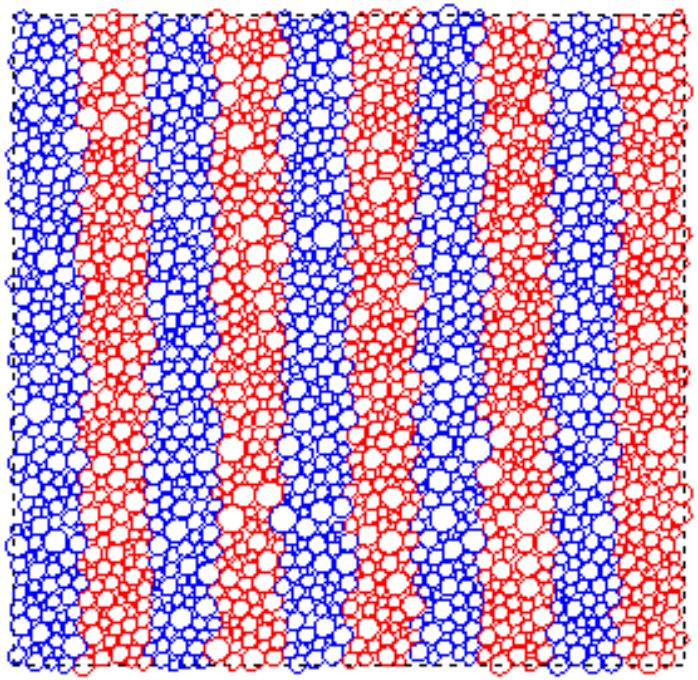

Macroscopic response

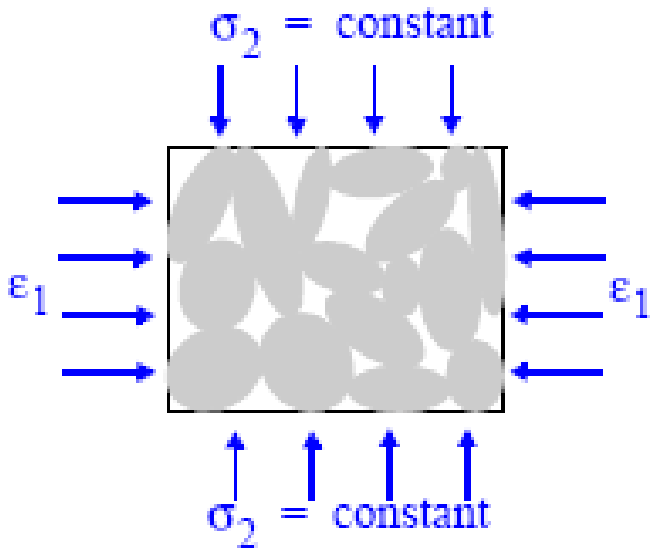

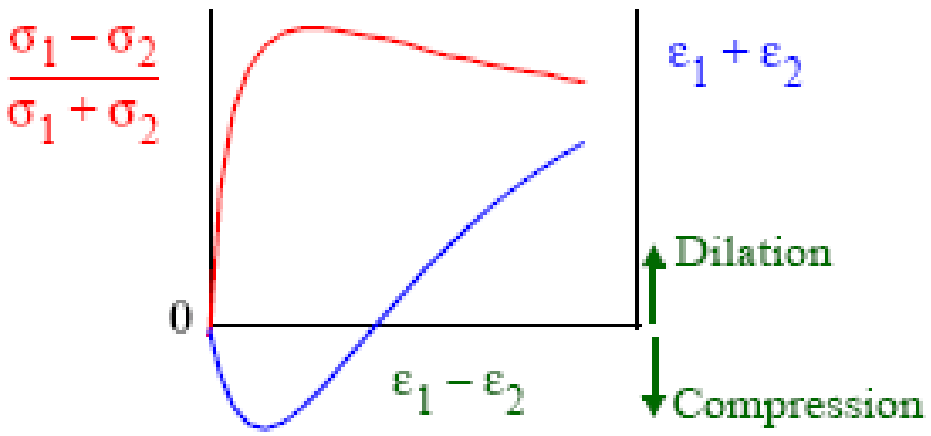

Fabric

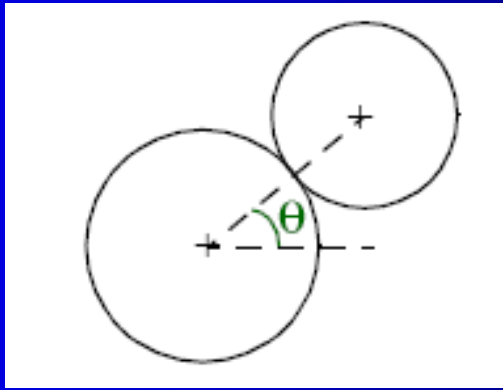

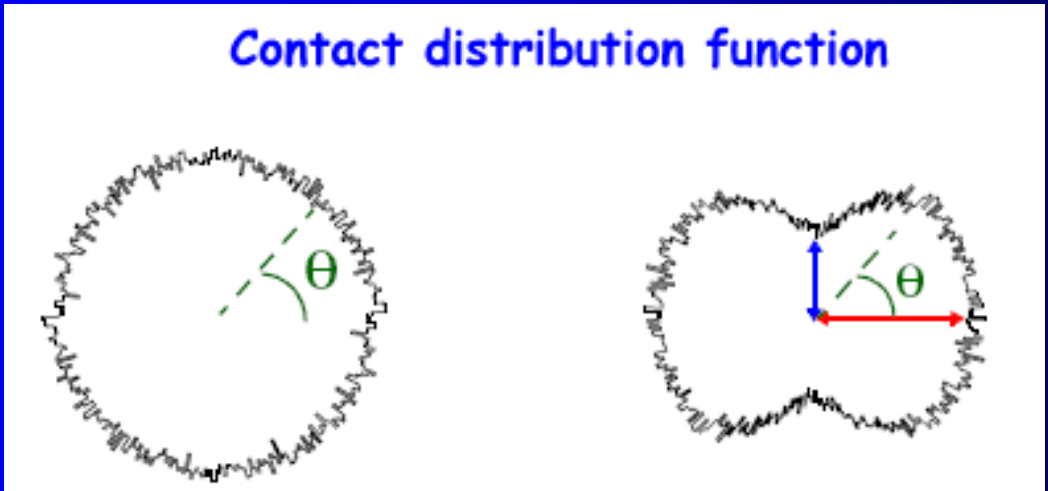

Induced anisotropy

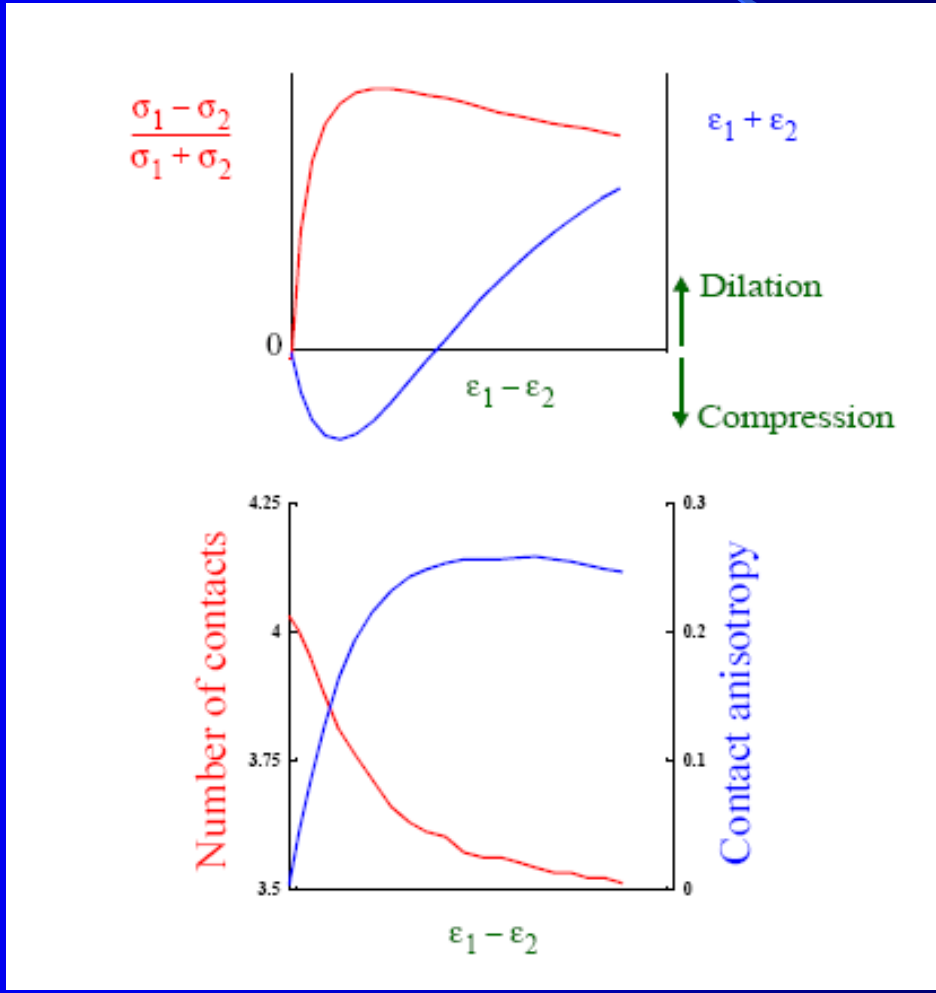

Force-fabric-strength (1)

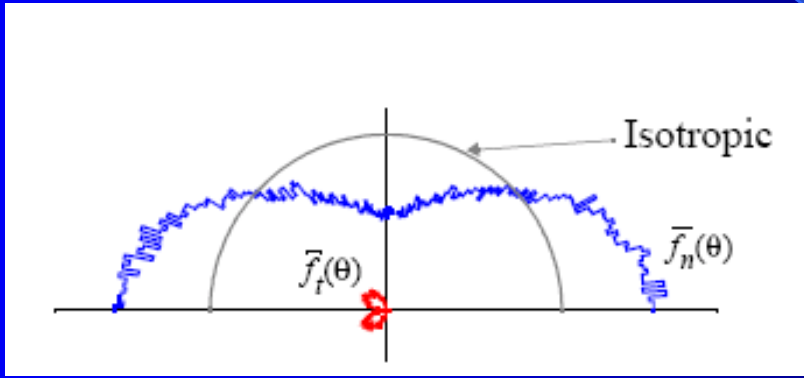

$$E(\theta)=\frac{1}{2\pi}\left[1+a_c\cos 2(\theta-\theta_0)\right]$$

$$\bar{f}_n(\theta)=f_0\left[1+a_n\cos 2(\theta-\theta_0)\right]$$

$$\bar{f}_t(\theta)=-a_t f_0\sin 2(\theta-\theta_0)$$

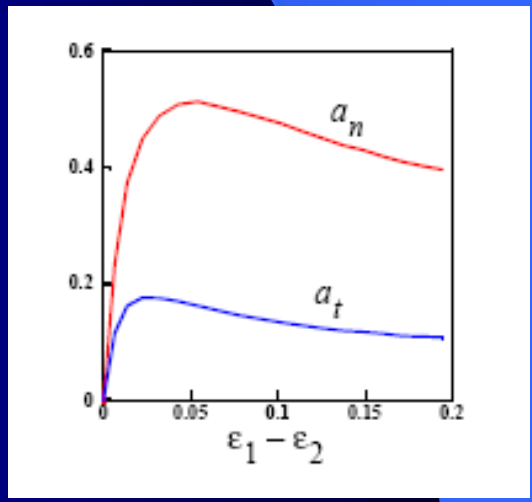

Force-fabric-strength (2)

$$\bar{\sigma}_{ij} = \frac{1}{V}\sum_{c\in C} l_i^c f_j^c = \frac{1}{V}\sum_{g}\sum_{c\in C_g} l_i^c f_j^c$$

$$\bar{\sigma}_{ij} = \frac{1}{V}\sum_{g} N_{c,g}\,\overline{l_i f_j}(\theta_g) \cong m_V \int_0^{2\pi} E(\theta)\bar{l}_i(\theta)\bar{f}_j(\theta)d\theta$$

$$\frac{\sigma_1 - \sigma_2}{\sigma_1 + \sigma_2} \cong \frac{1}{2}\left[a_c + a_n + a_t\right]$$

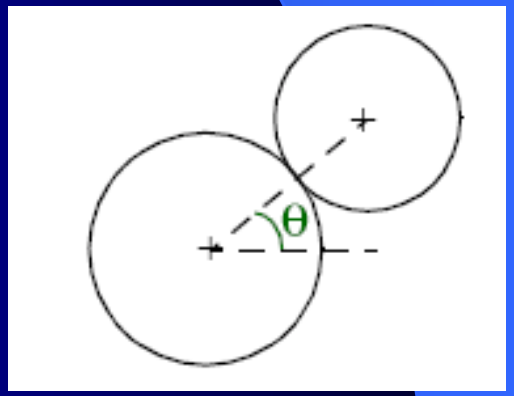

Effect of interparticle friction on macroscopic behaviour

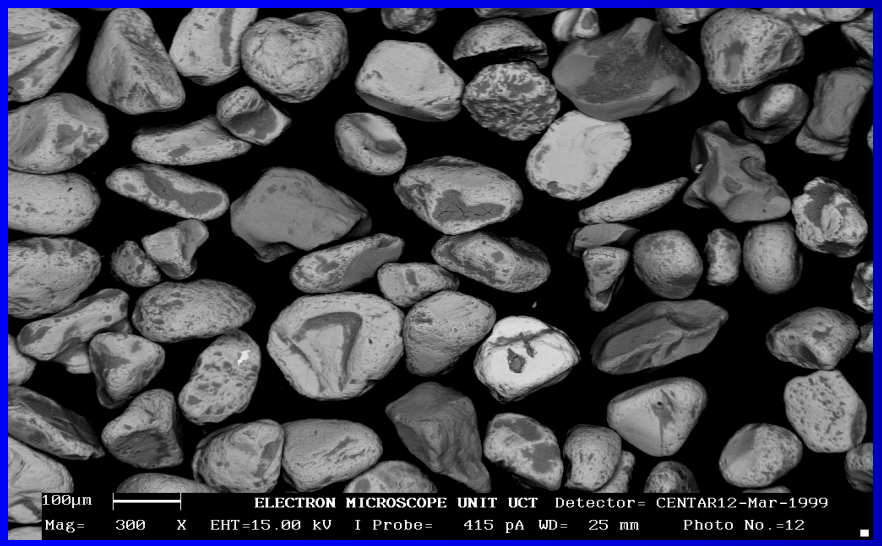

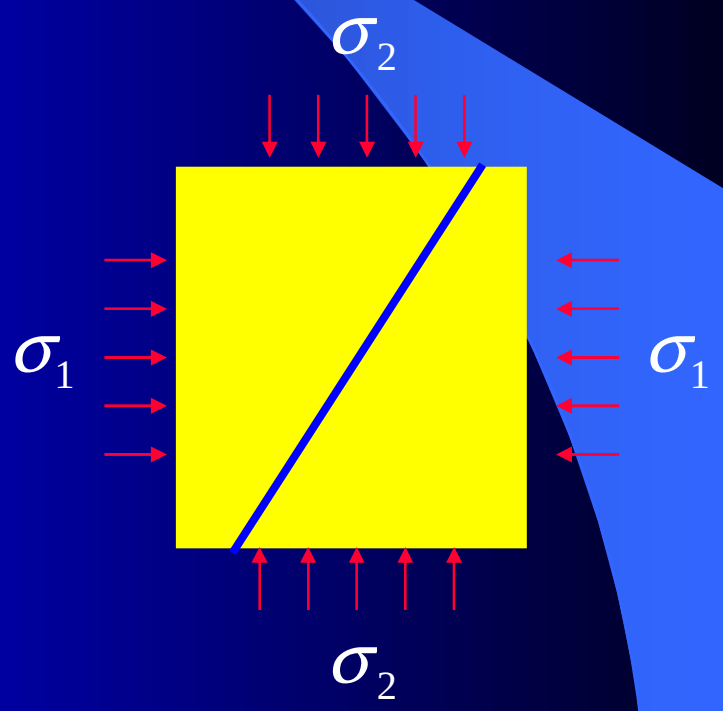

Granular materials are frictional (1)

Microscopic (contact) frictional behaviour

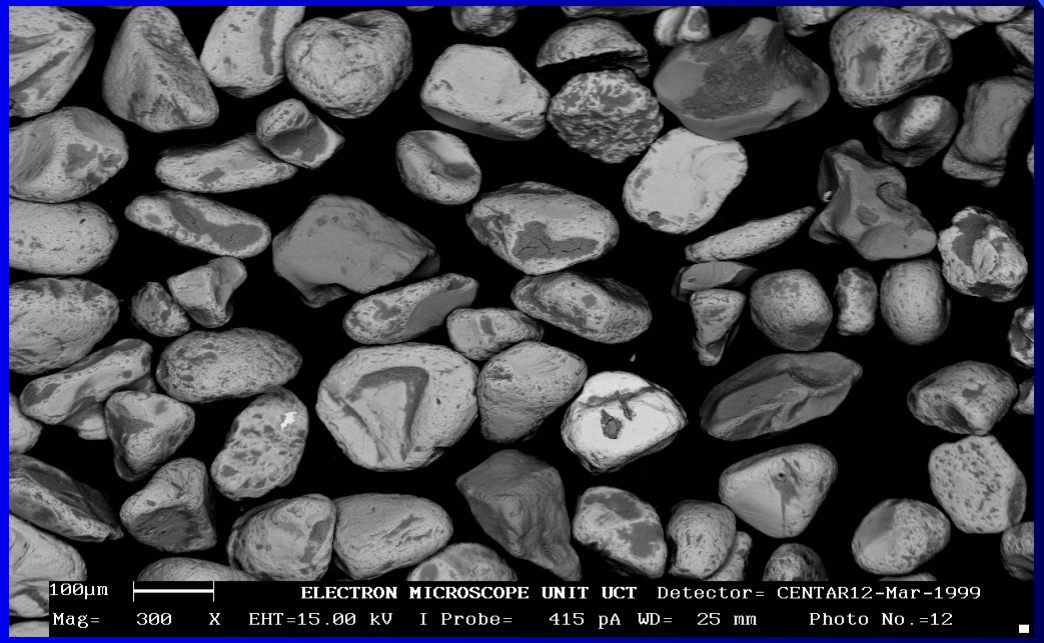

Granular materials are frictional (2)

Macroscopic (continuum) frictional behaviour

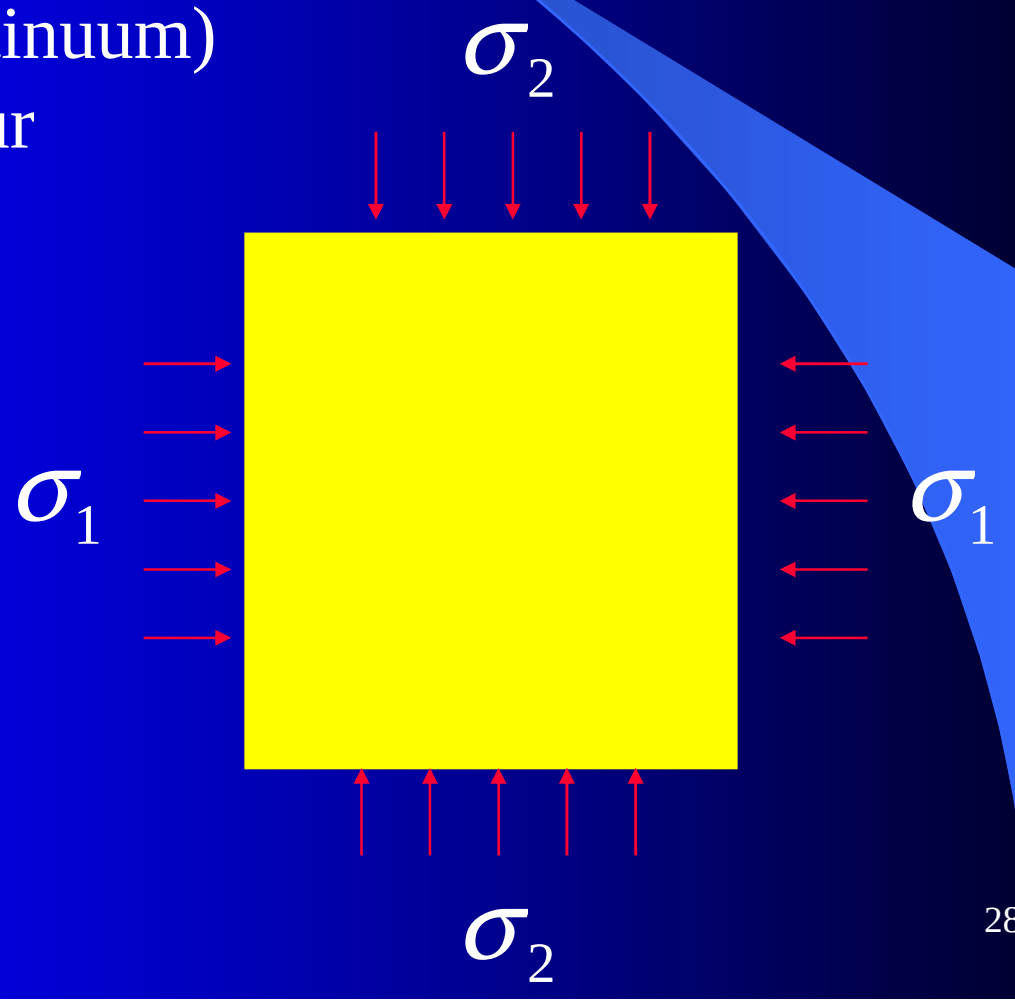

Correlations between microscopic and macroscopic friction

Horne (1965)

$$\tan^2\left(\frac{\pi}{4}+\frac{1}{2}\phi_{peak}\right)=2\tan\left(\frac{\pi}{4}+\phi_{\mu}\right)$$

Bishop (1954)

$$\sin\phi_{\infty}=\frac{15\tan\phi_{\mu}}{10+3\tan\phi_{\mu}}$$

Weak dependence of macroscopic friction on microscopic friction:

$$\mu=\tan\phi_{\mu}$$

- experimentally (Skinner, 1969)
- numerically (Cambou, 1993)

Influence μ

- shear strength
- dilatancy
- energy
- dissipation

Shear strength and dilatancy

Shear strength

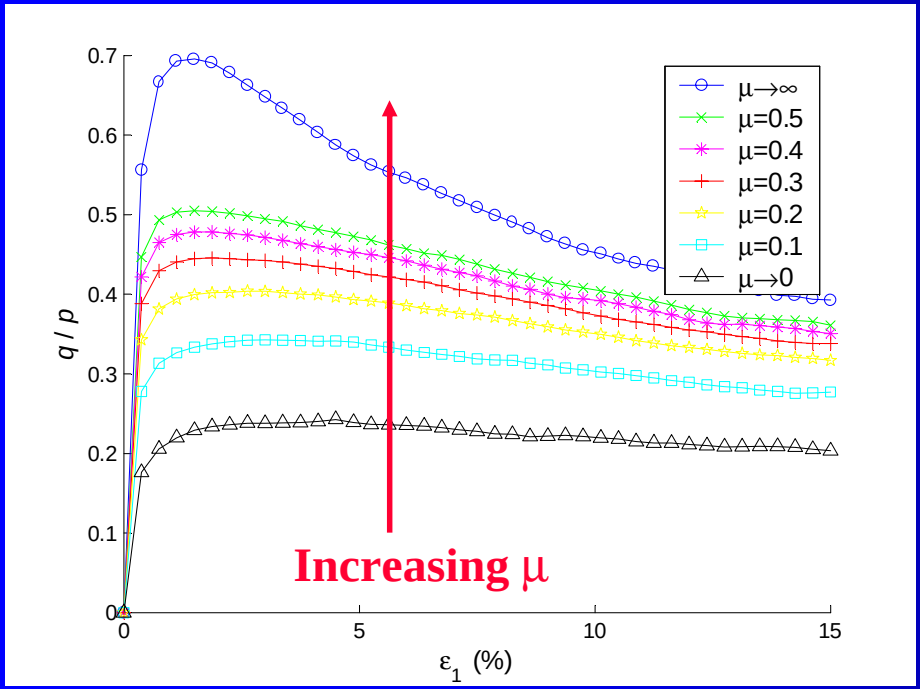

Dilatancy

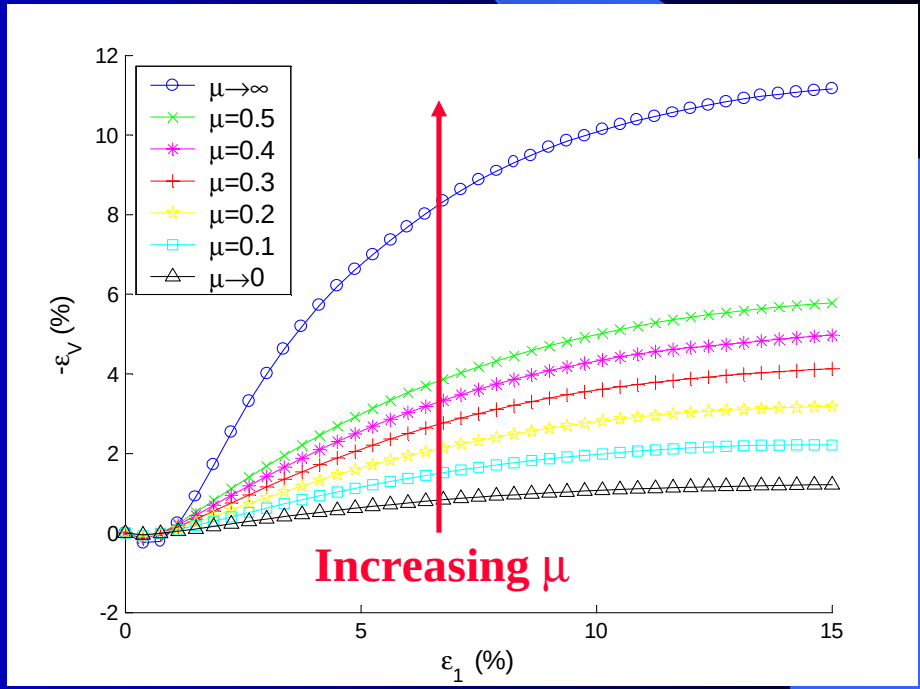

Plastic strains: unloading paths

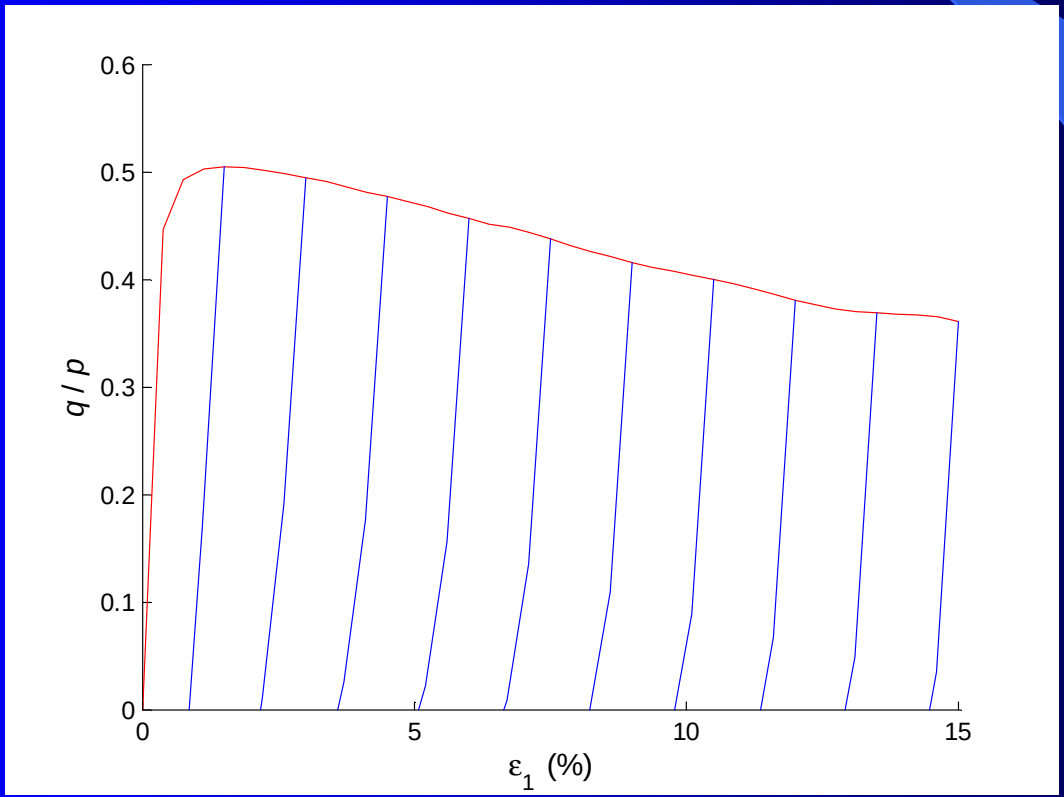

Dilatancy rate $-\frac{d\varepsilon_V^p}{d\varepsilon_S^p}$

Formulated in *plastic* strains

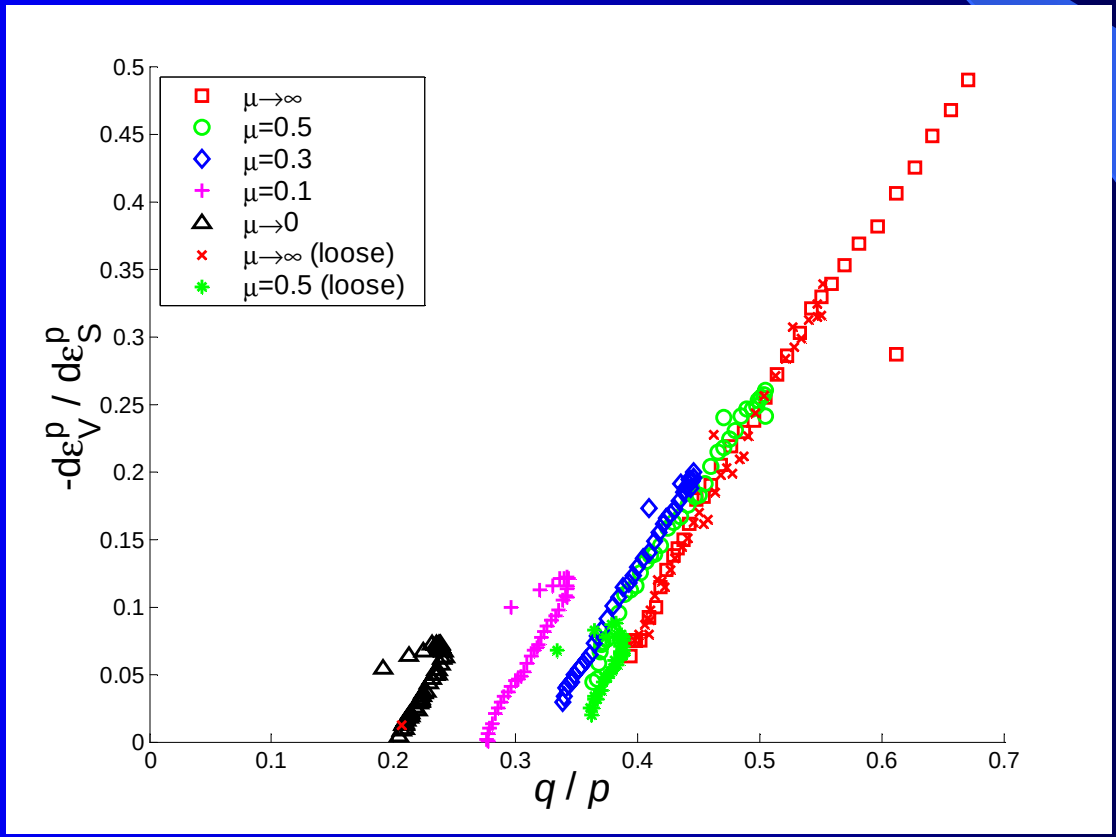

Strength at peak & steady-state, dilatancy rate at peak strength

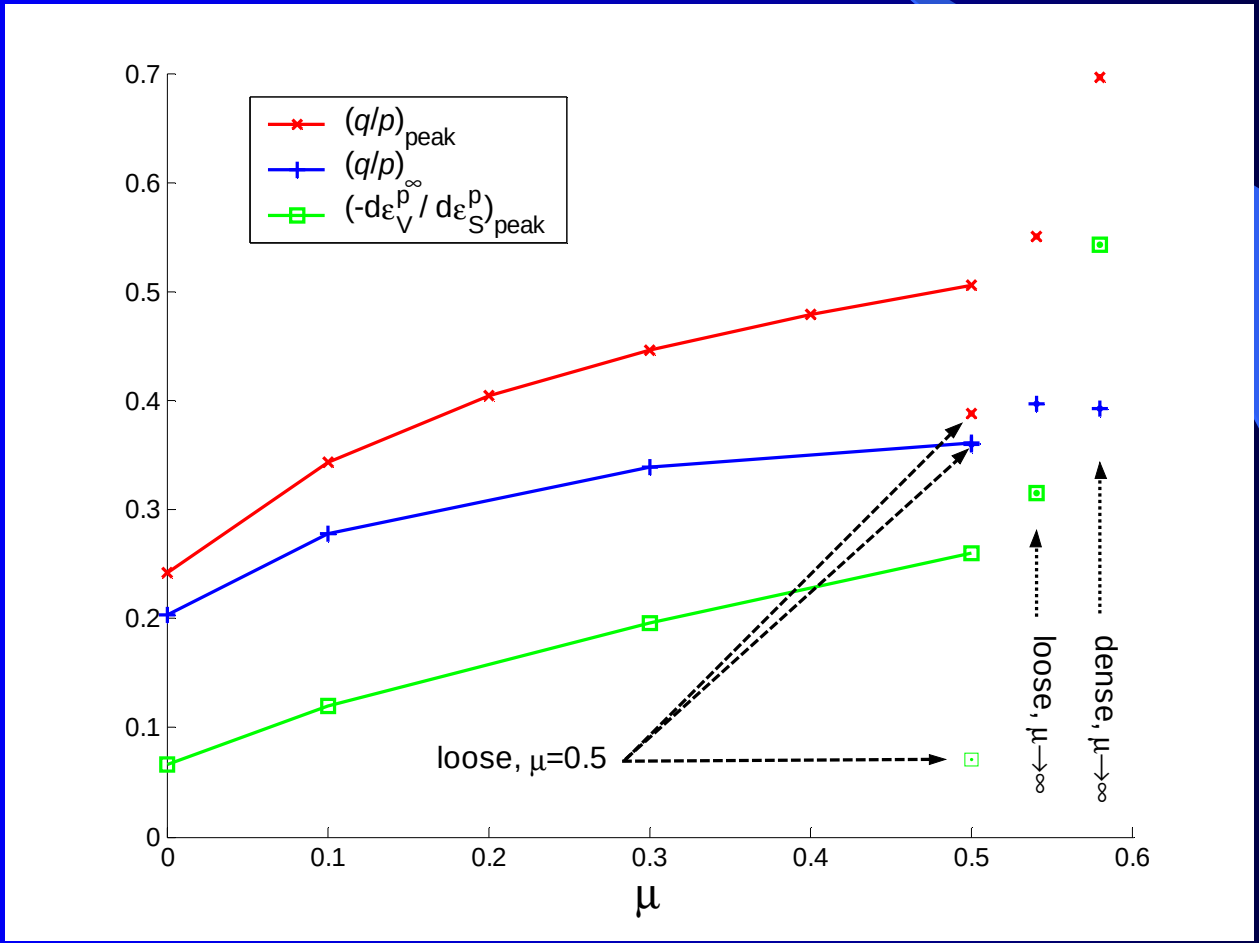

Strength-dilatancy relation

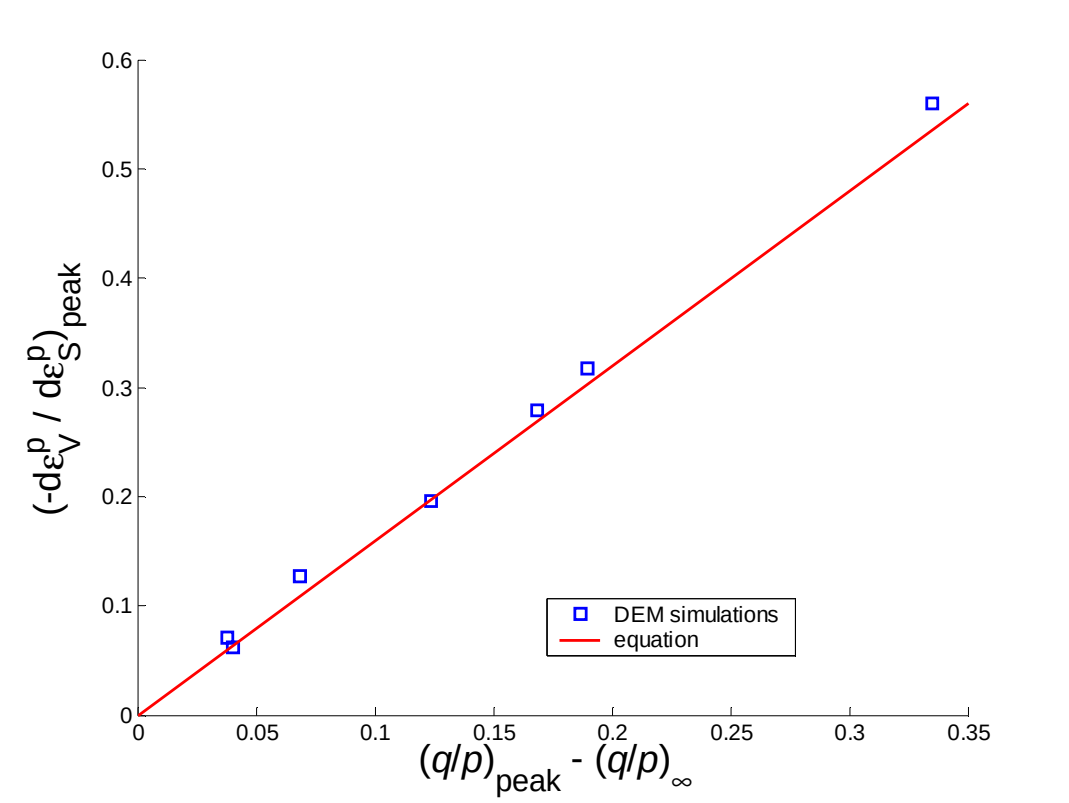

$$\left(-\frac{d\varepsilon_V^p}{d\varepsilon_S^p}\right)_{\text{peak}} = \alpha\left[(q/p)_{\text{peak}} - (q/p)_\infty\right]$$

Strength correlations vs. simulations

Peak strength

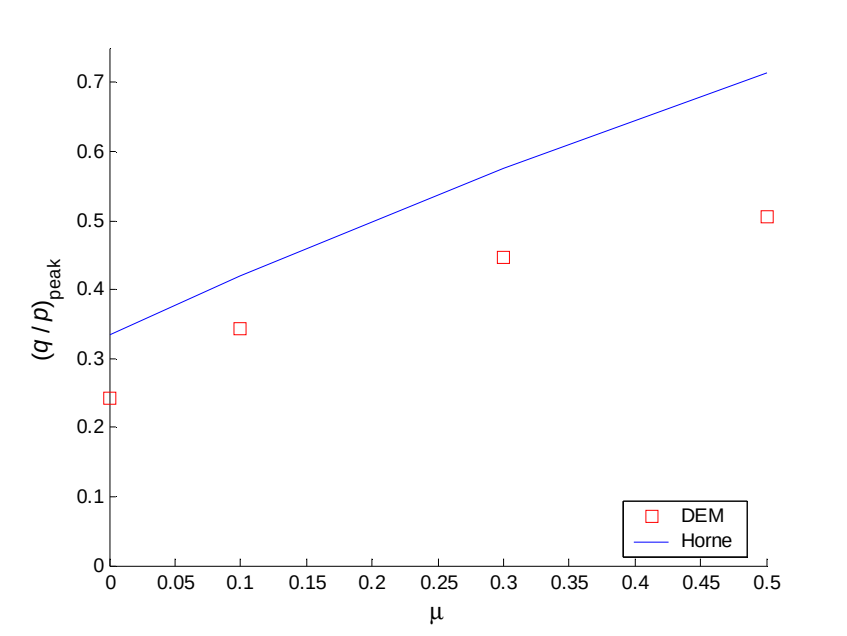

Steady-state strength

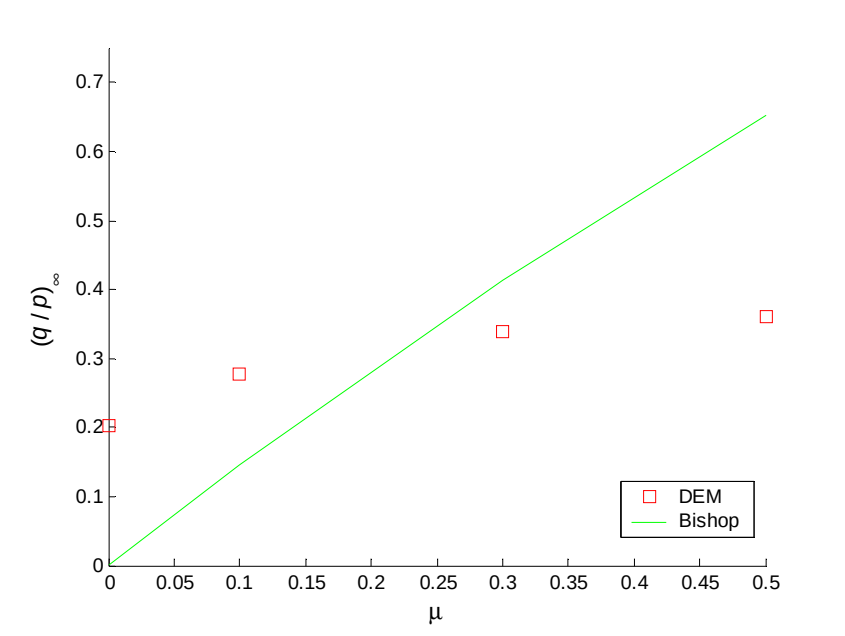

Energy

$$U_n = \frac{1}{V}\sum_{c\in C}\frac{1}{2k_n}\left[f_n^c\right]^2 \qquad U_t = \frac{1}{V}\sum_{c\in C}\frac{1}{2k_t}\left[f_t^c\right]^2$$

$$U = U_n + U_t$$

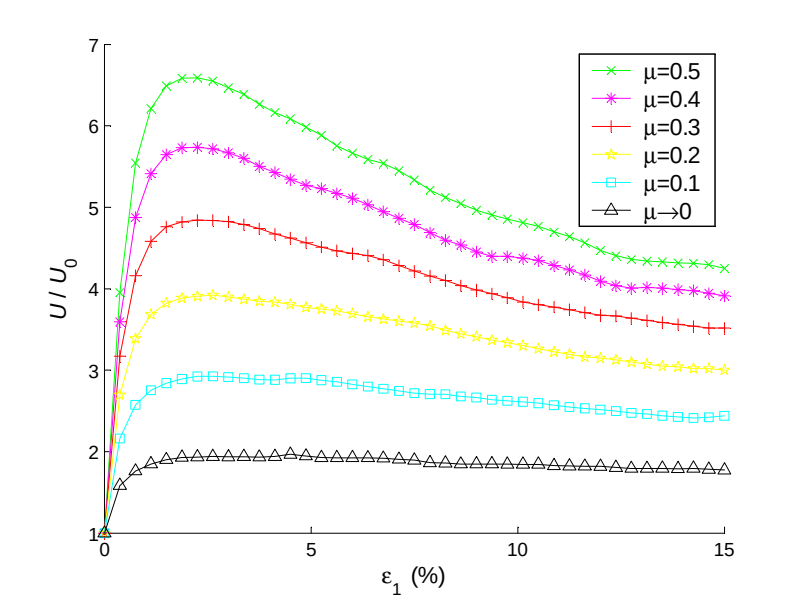

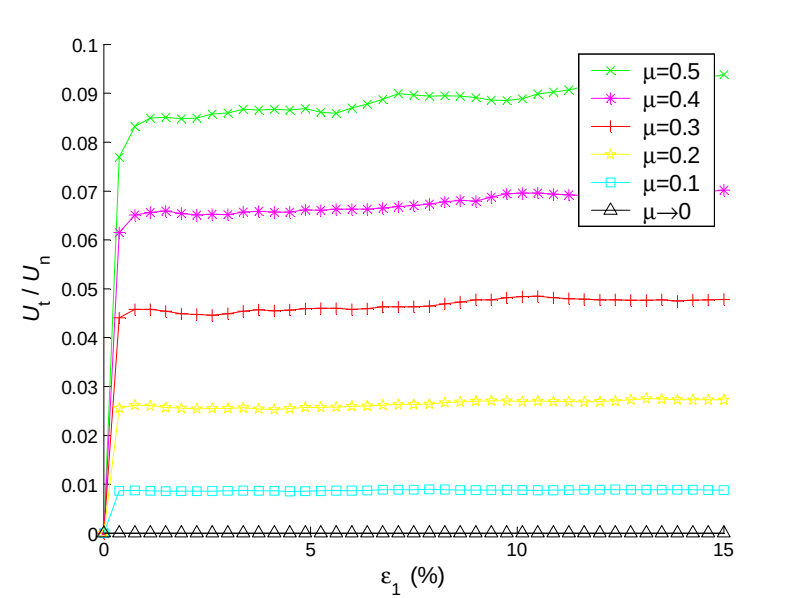

Dissipation

Dissipation

Work input

Change in energy

$$\delta D \cong \delta W - dU$$

$$= \sigma_{ij} d\varepsilon_{ij} - dU$$

Dissipation

Dissipation | Work input | Change in energy

$$\delta D \cong \delta W - dU$$

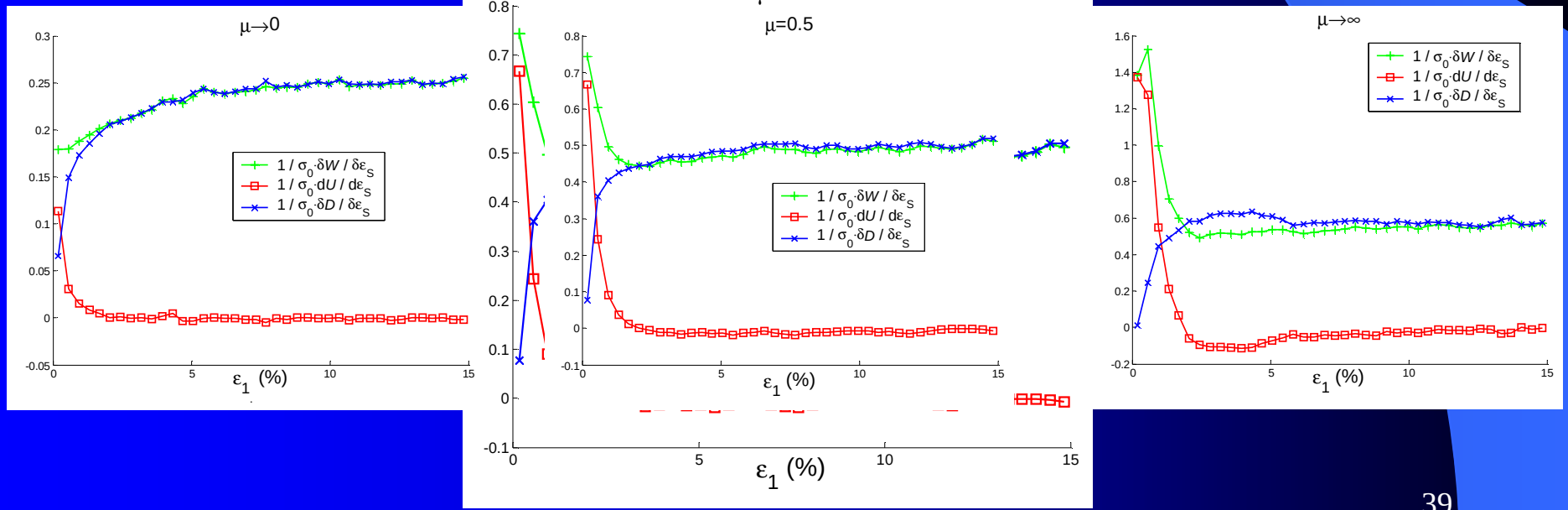

Dissipation function

Work inpu

Strength-d

$p)_\infty]$

Resulting dissipation function:

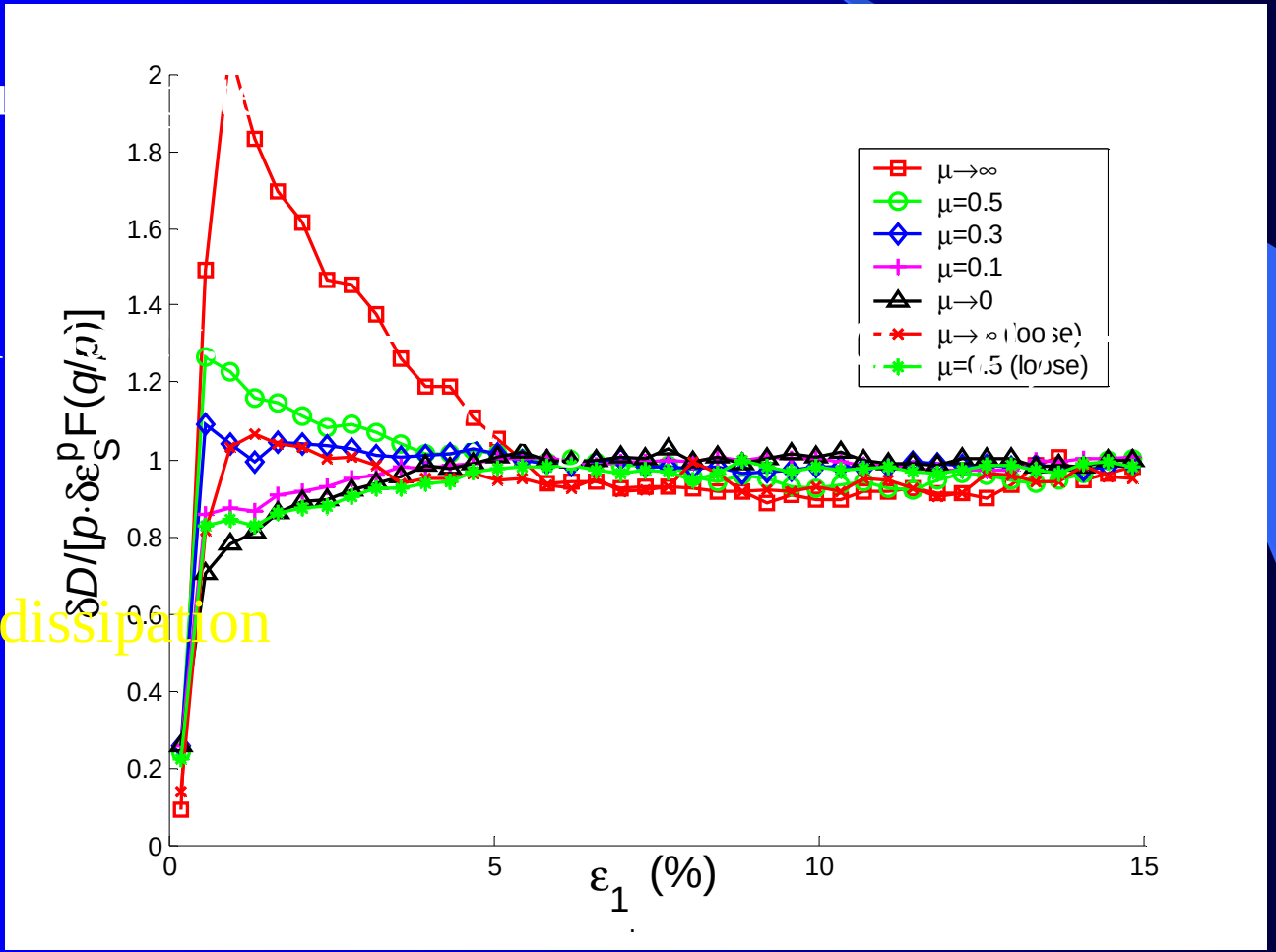

Conclusions

- For all μ, frictional behaviour at macro-level
- Macro-level dissipation, even for $\mu \rightarrow 0$ and $\mu \rightarrow \infty$

- Strength-dilatancy relation
- Constant ratio of ‘tangential’ over ‘normal’ energy beyond initial range
- All work input is dissipated beyond initial range

Discussion

- Origin of macroscopic frictional behaviour:
  - Interparticle friction: NO
  - Contact disruption and creation: POSSIBLY
- Origin of dissipation if $\mu \rightarrow 0$ or $\mu \rightarrow \propto$:
  - Dynamics & restitution coefficient
  - Microscopic restitution coefficient $\Rightarrow$ macroscopic plastic dissipation

Summary

- Slow flows
- Stress and strain
- Frictional nature
- Geometrical anisotropy
- Validity mean-field approximation

Mixing of granular materials in rotating cylinders

Niels P. Kruyt

Department of Mechanical Engineering,
University of Twente

n.p.kruyt@utwente.nl
www.ts.ctw.utwente.nl/kruyt/

Co-workers

- Gerard Finnie:
  - Mineral Processing Group, University of Witwatersrand, Johannesburg, South Africa
- Mao Ye & Christiaan Zeilstra & Hans Kuipers:
  - Department of Chemical Engineering, University of Twente

Mixing in rotating cylinders

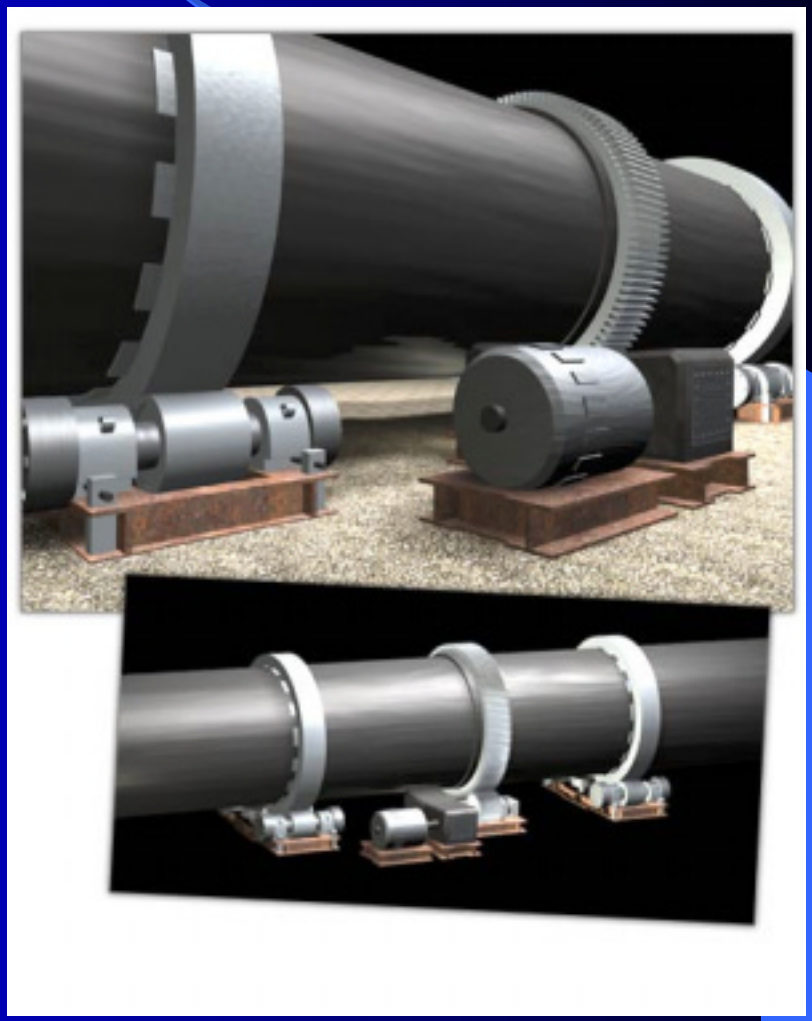

Functions of rotary kilns

- Mixing
- Calcination
- Drying
- Waste incineration

…

Process parameters

- Speed of rotation, Ω
- Radius, *R*
- Filling degree, *J*
- Length, *L*

- Material properties
- Inclination
- Gas flow

…

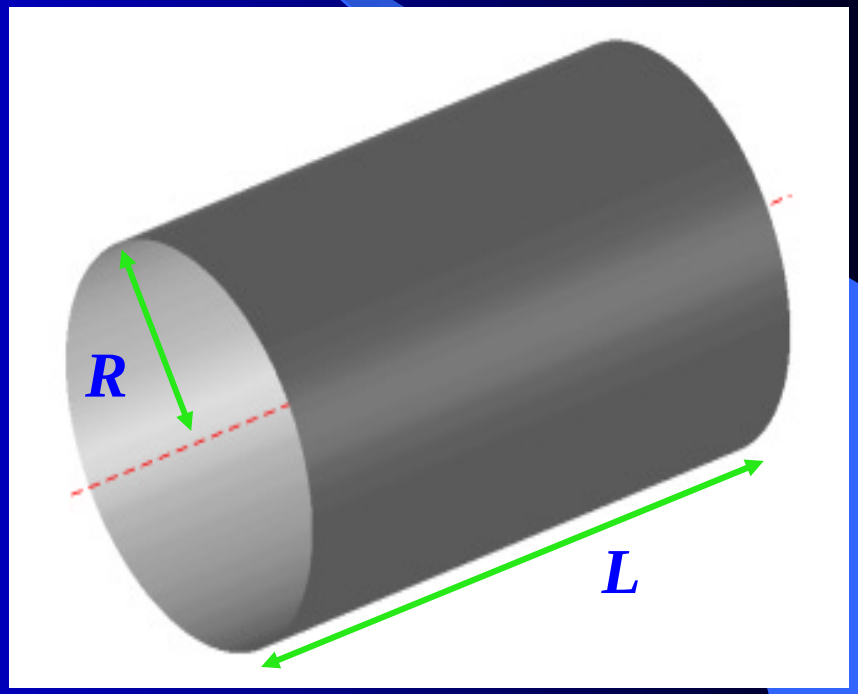

Flow regimes

Increasing rotational speed

Basic form	Slipping motion		Cascading ("tumbling") motion			Cataracting motion	
Subtype	Sliding	Surging	Slumping	Rolling	Cascading	Cataracting	Centrifuging
Schematic	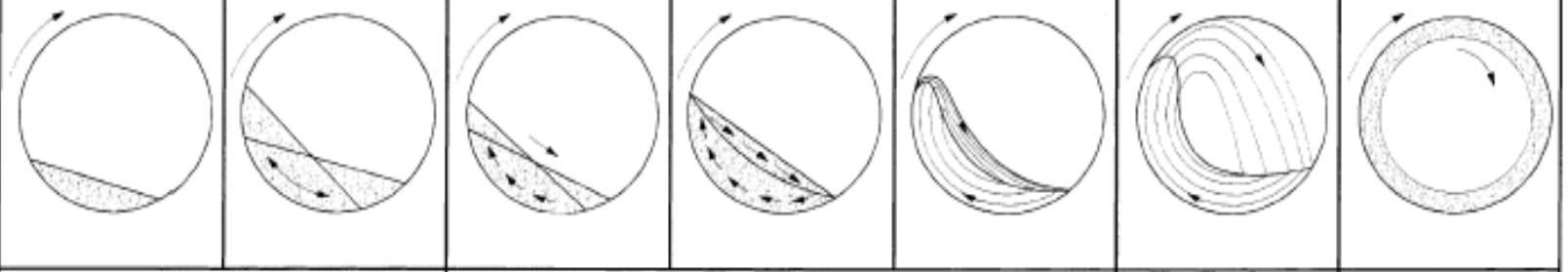						
Physical process	Slipping		Mixing			Crushing	Centrifuging

From: Mellmann, Powder Technology (2001)

Mixing in rotary kilns

- Transverse $\rightarrow$ fast
- Longitudinal $\rightarrow$ slow

- Fascinating patterns

From: Shinbrot et al., Nature (1999)

Segregation

- Separation due to differences in:
  - Size
  - Density
- Transverse & longitudinal segregation
- Here *no* segregation:
  - Equal densities
  - Small size differences

Dependence of mixing on process parameters

- Non-dimensional parameters
  - Froude number $Fr = \frac{\Omega^2 R}{g}$
  - Filling degree J

Approach: Discrete Element Method

- Many-particle simulation method
- Numerics: explicit time-stepping of equations of motion
  - displacements
  - rotations
- simple models at micro level $\rightarrow$ complex behaviour at macro level

Contact constitutive relation

- Elastic
- Frictional
- Damping

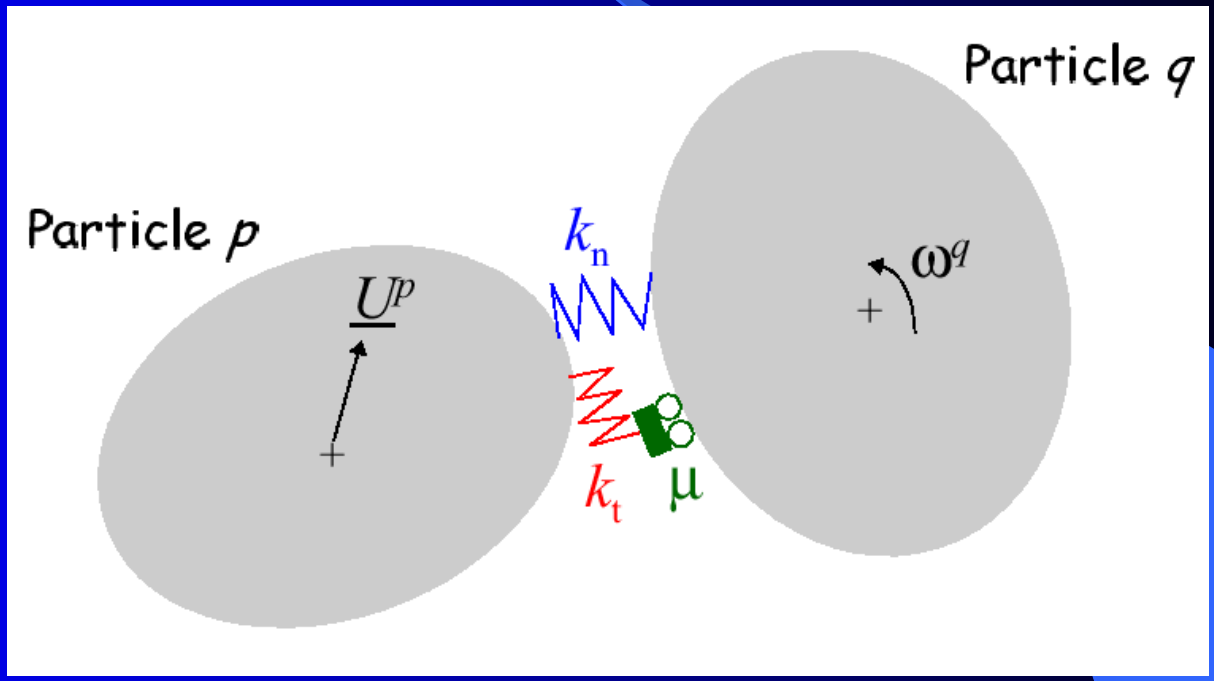

Velocities

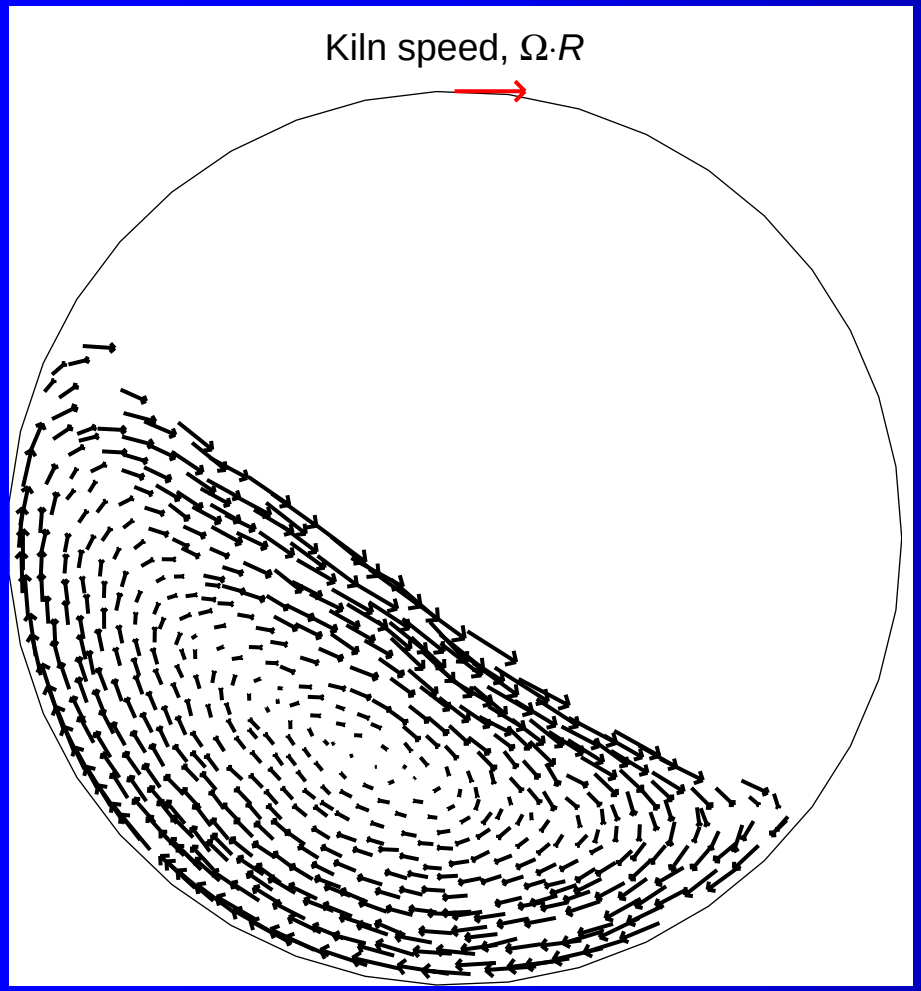

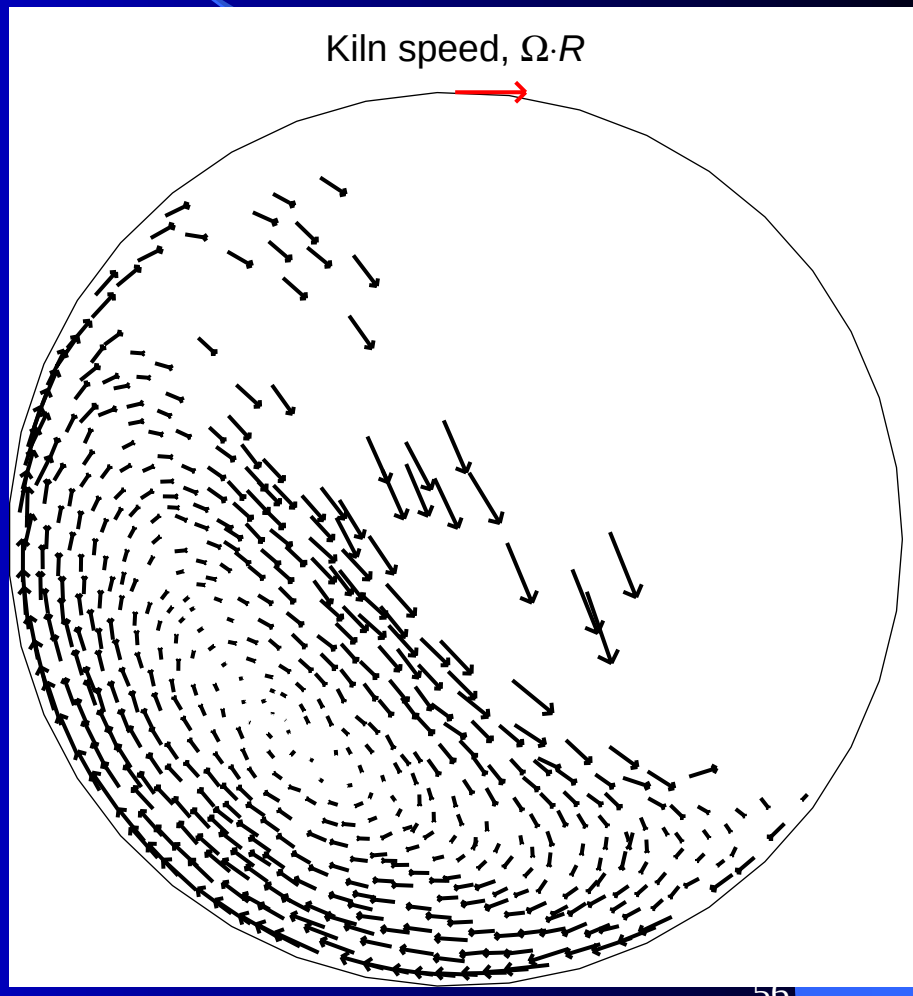

Visualization: 2D

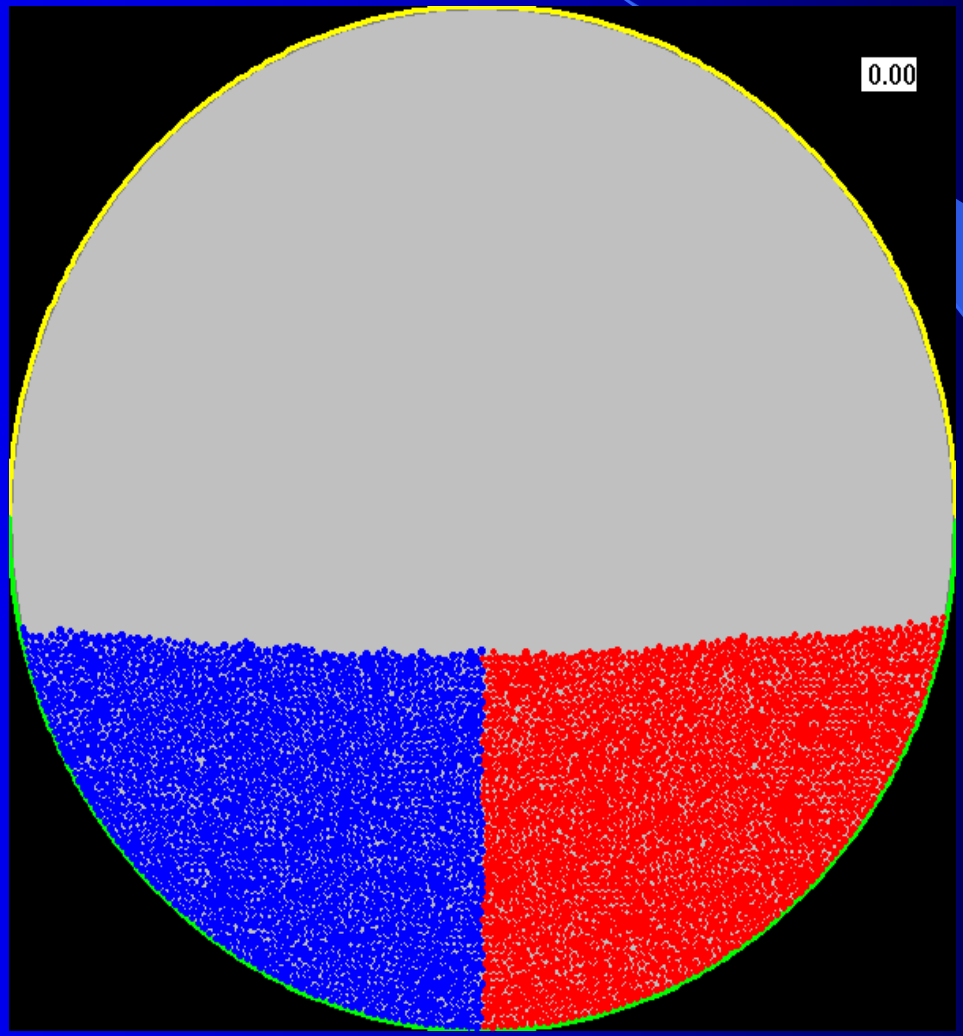

Visualizations: effect of *Fr*

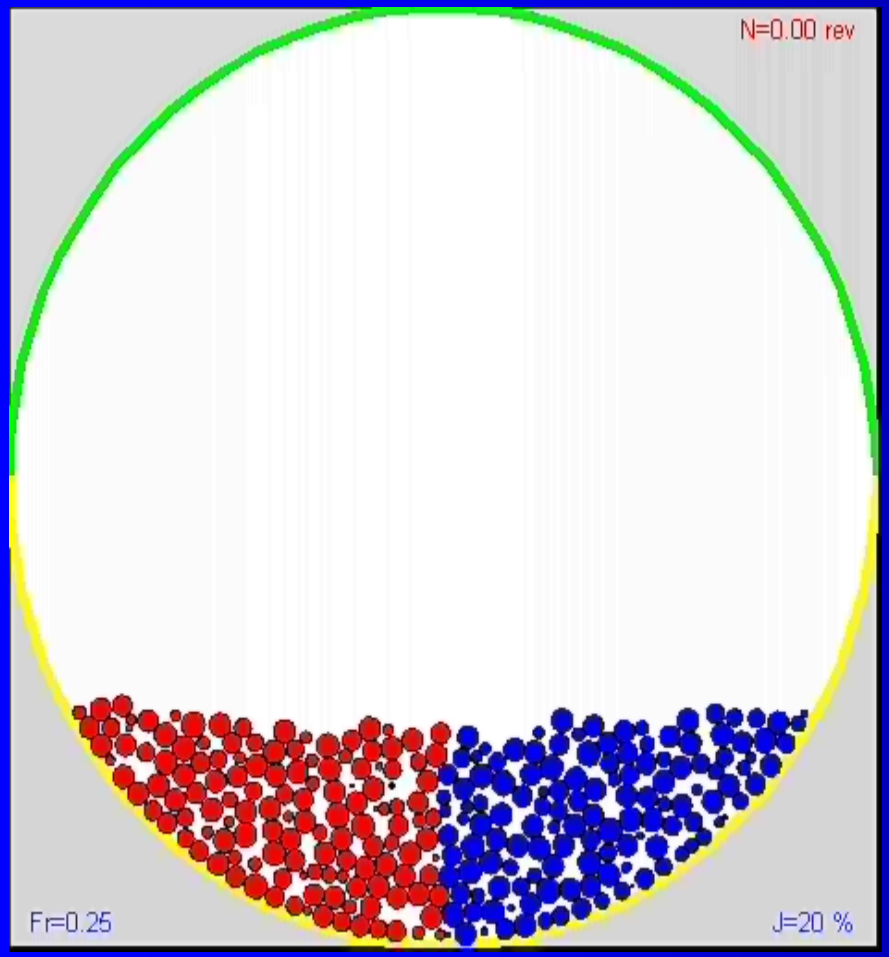

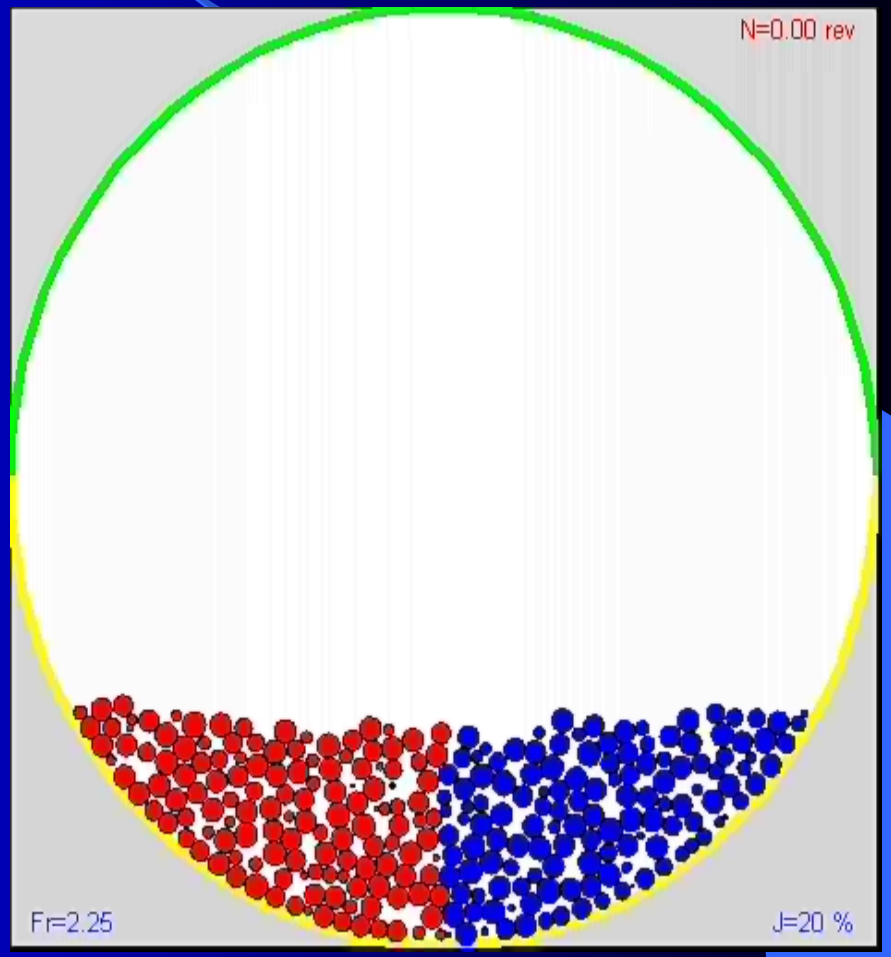

Visualizations: effect of *J*

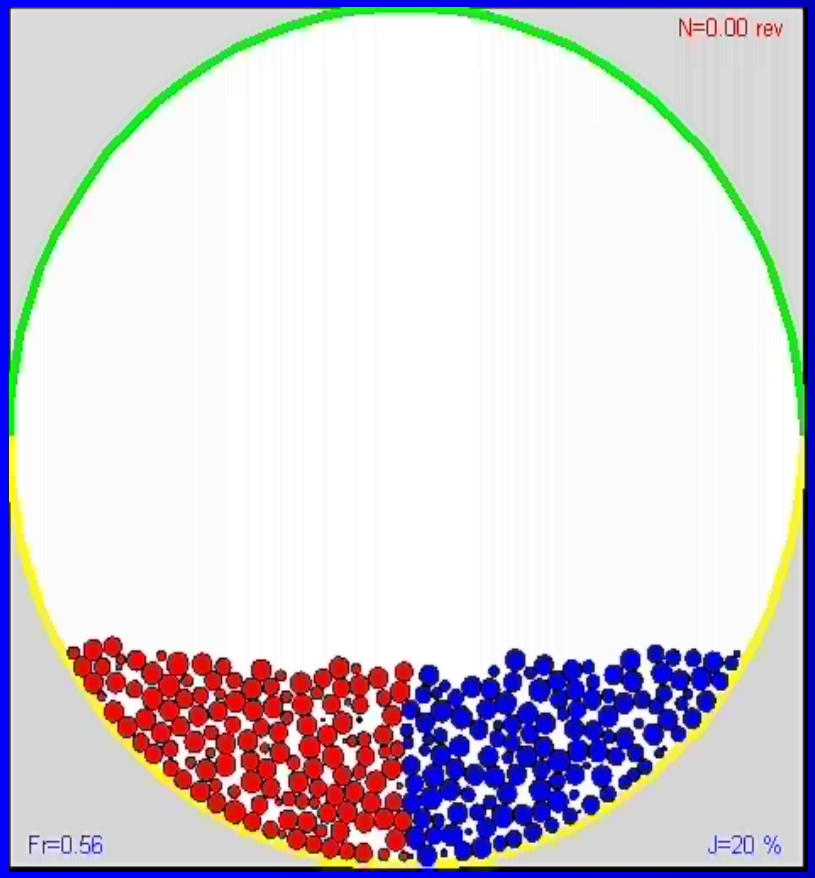

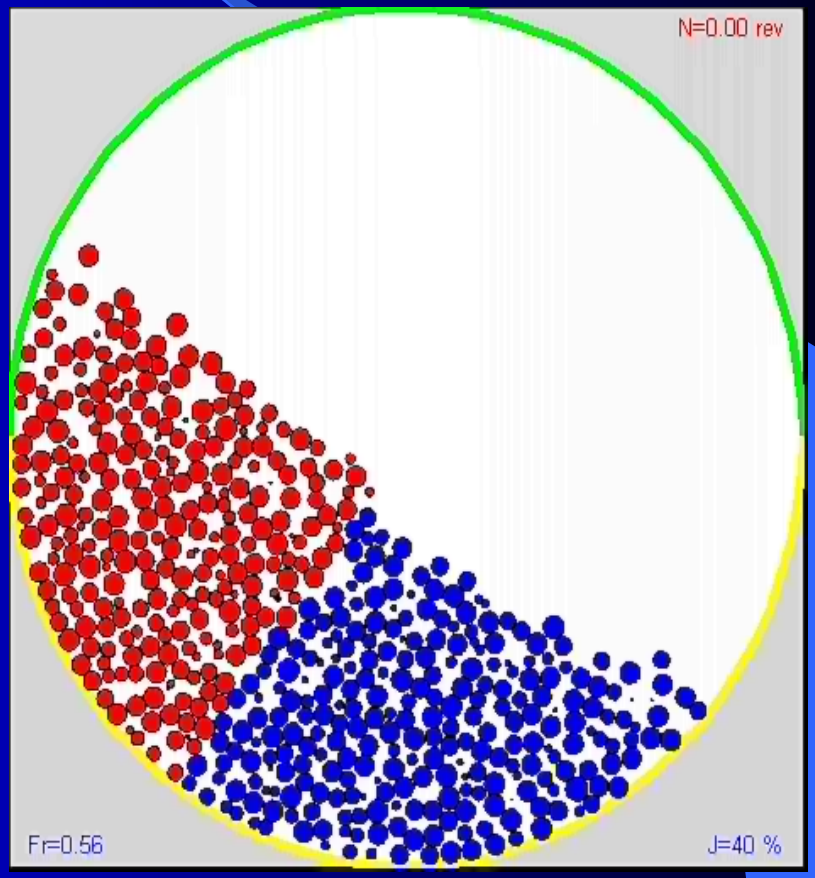

Longitudinal mixing

- Diffusion process; no throughflow

$$\frac{\partial c}{\partial n} = D\frac{\partial^2 c}{\partial x^2} \qquad \frac{\partial c}{\partial t} = D^*\frac{\partial^2 c}{\partial x^2} \qquad D^* = \frac{D\Omega}{2\pi}$$

- Solution

$$c(x,n) = \frac{1}{2} + \sum_{j=1}^{\infty} \frac{1}{2j-1} \exp\left(-\frac{(2j-1)^2\pi^2 Dn}{L^2}\right) \sin\frac{(2j-1)\pi n}{L}$$

Determination of diffusion coefficient (1)

- Mean position of “red” particles

$$X_R(n) = \frac{1}{L}\int_{-L/2}^{+L/2} xc(x,n)dx$$

- For small “Fourier” number

$$X_R(n) \cong \frac{1}{4} - 2\left(\frac{Dn}{L^2}\right)$$

Determination of diffusion coefficient (2)

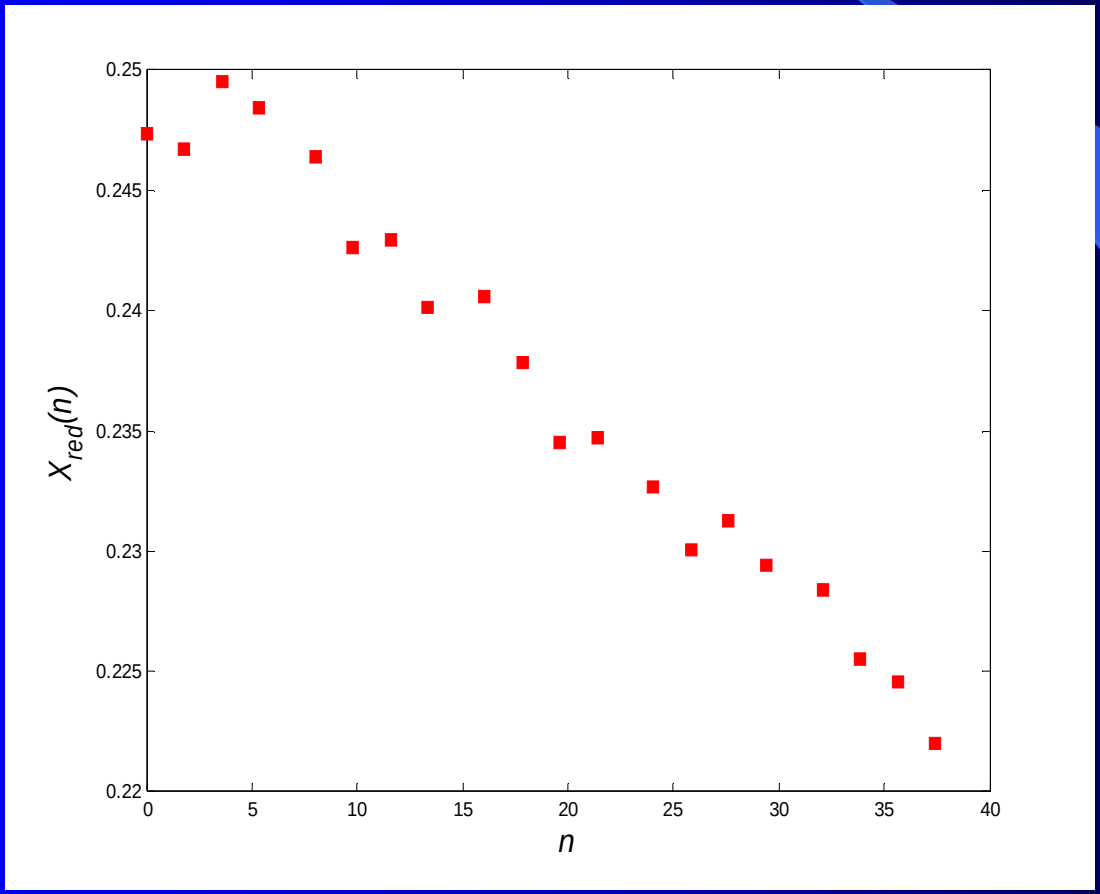

Linear relation is indeed observed!

Concentration profiles

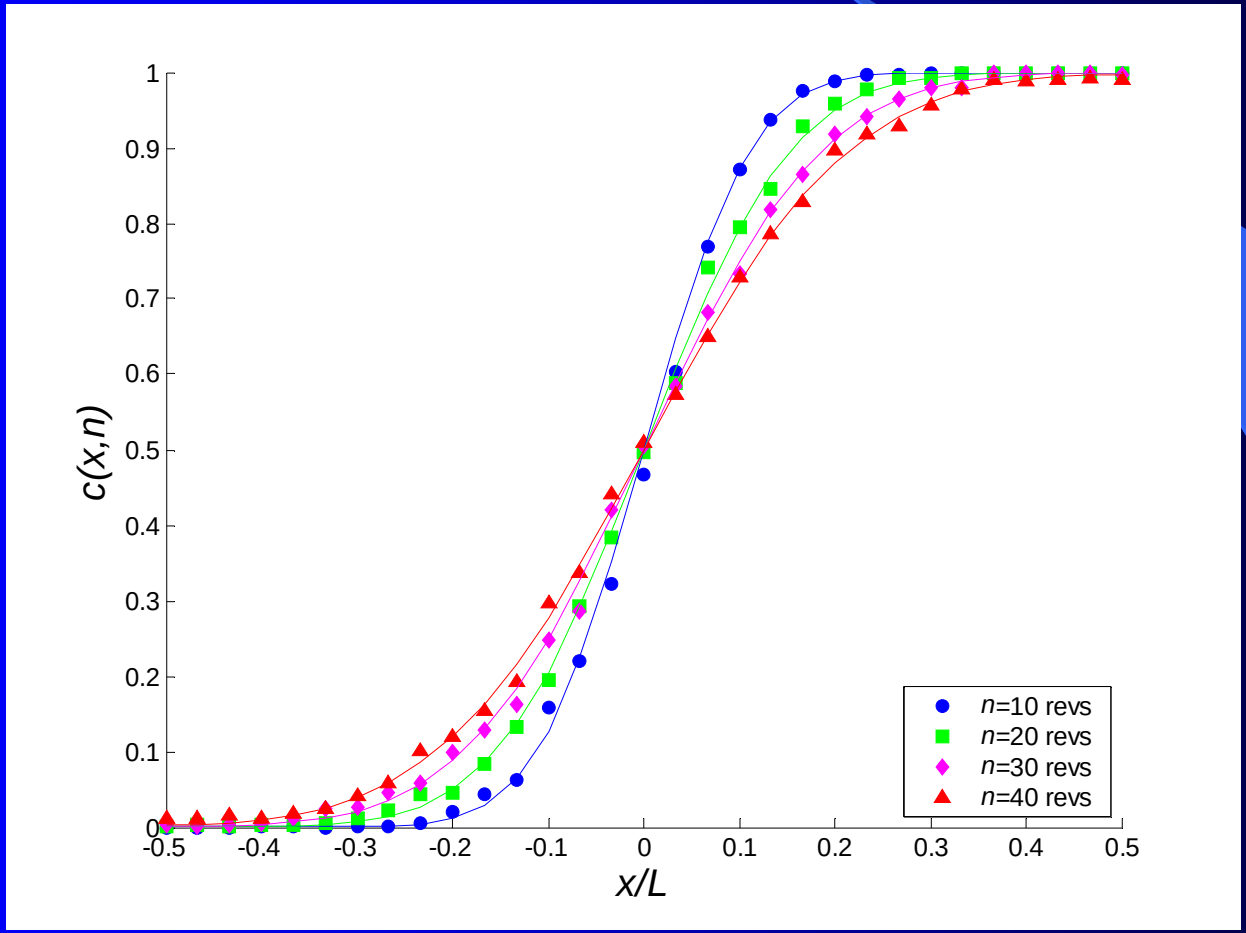

Dependence of diffusion coefficient on process parameters

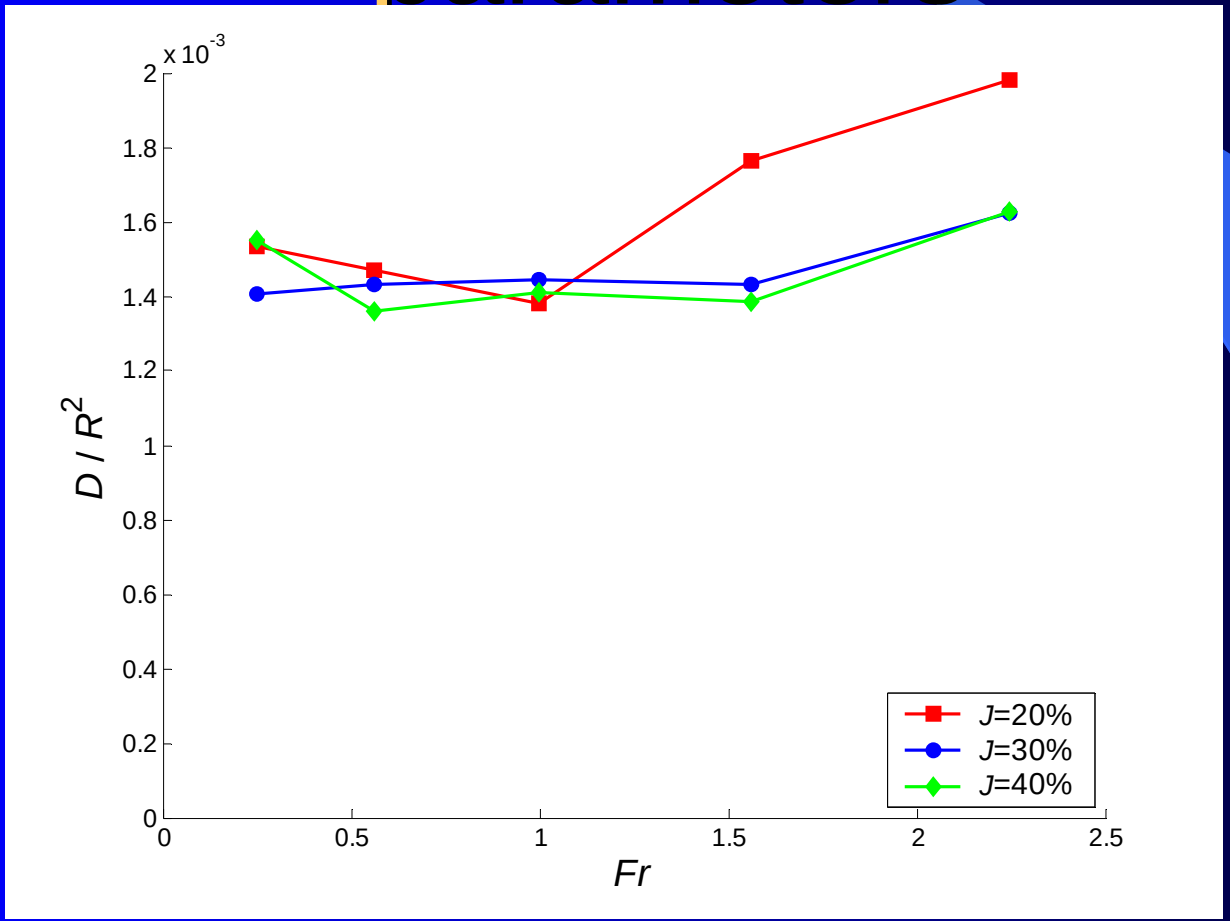

Comparison with other studies

- Present $D^* \propto \Omega^{1.0}$
- Dury & Ristow (1999) $D^* \propto \Omega^{2.0}$
- Rao et al. (1991) $D^* \propto \Omega^{1.0}$
- Rutgers (1965) $D^* \propto \Omega^{0.5}$
- Sheritt et al. (2003) $D^* \propto \Omega^{0.4}$

$$D = \text{const}$$

$$D^* = \frac{D\Omega}{2\pi}$$

Transverse mixing: initial configuration

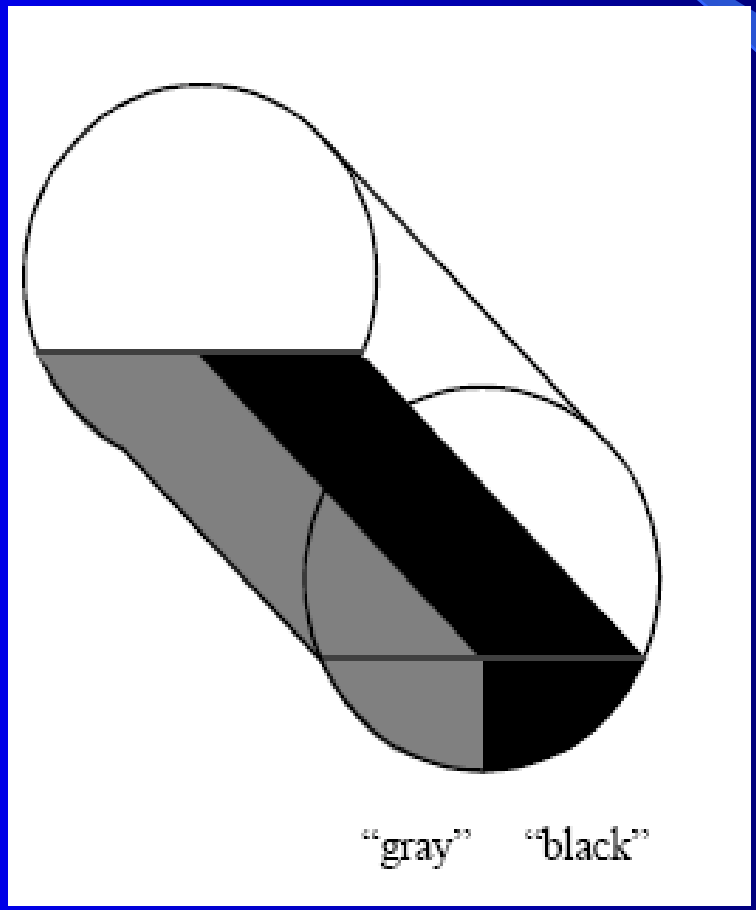

Transverse mixing

- Entropy-like mixing index

$p_{i,j}$: fraction of "black" particles

$q_{i,j}$: fraction of "gray" particles

$$I_{i,j} = -kV_{i,j}\left(p_{i,j}\ln p_{i,j} + q_{ij}\ln q_{i,j}\right)$$

$$M(n) = \sum_{i,j}\frac{I_{i,j}(n)}{I(n\to\infty)}$$

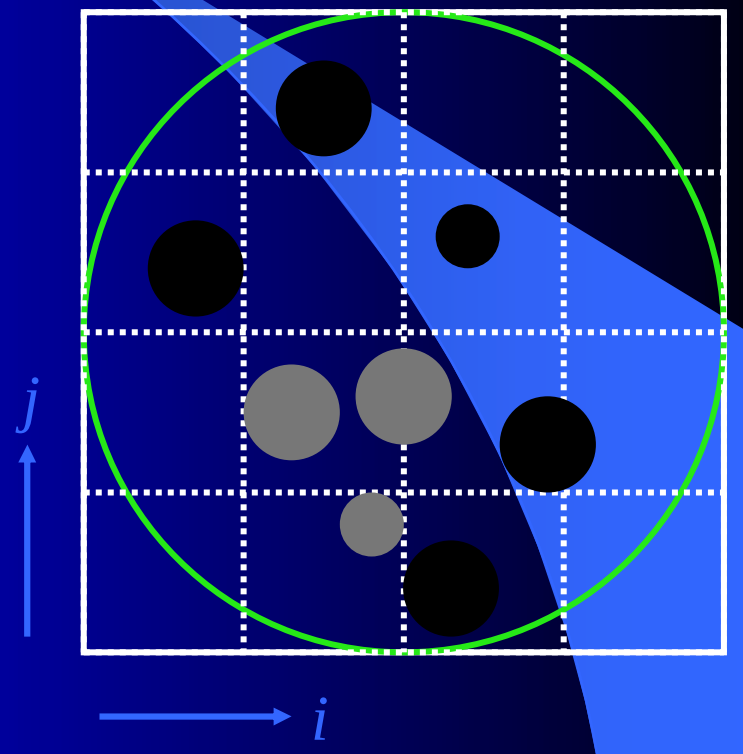

Evolution of mixing index

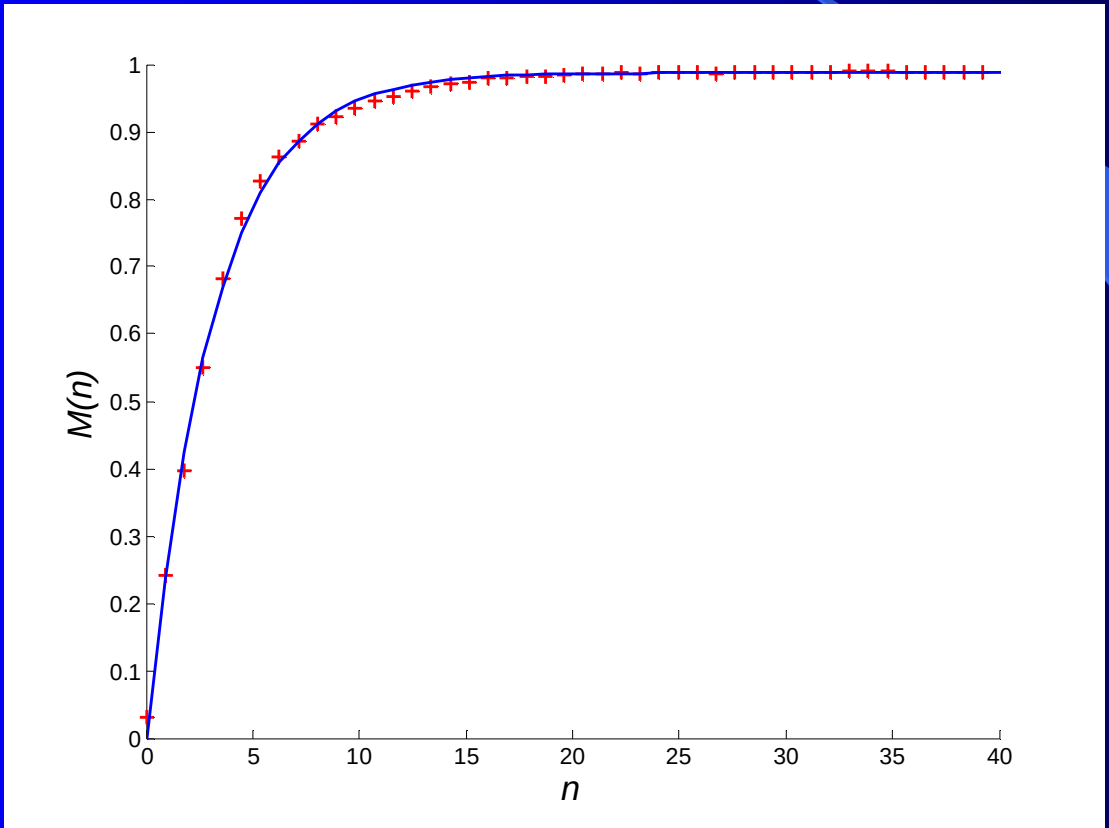

$$M(n) \cong 1 - \exp(-Sn)$$

Mixing speed

Dependence of mixing speed on process parameters

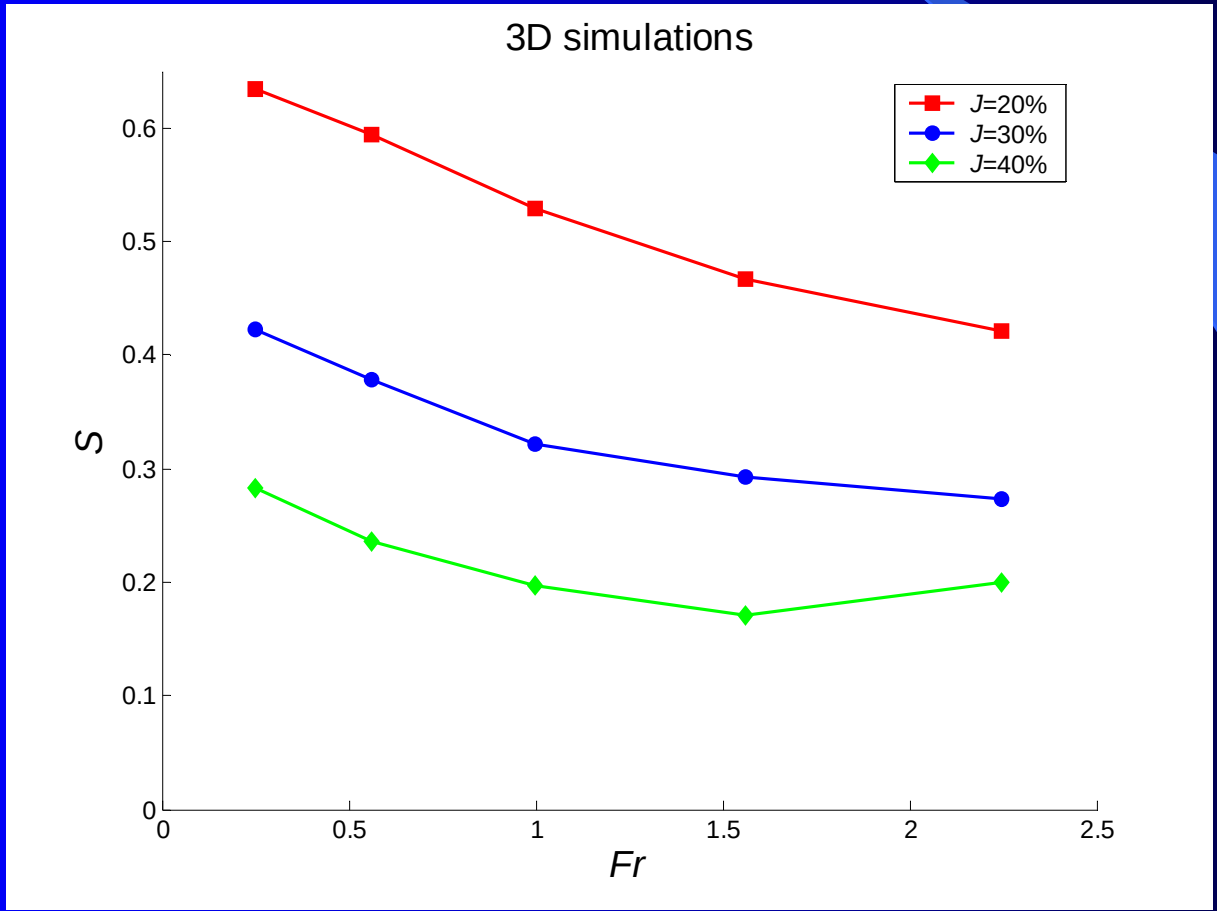

2D vs. 3D simulations

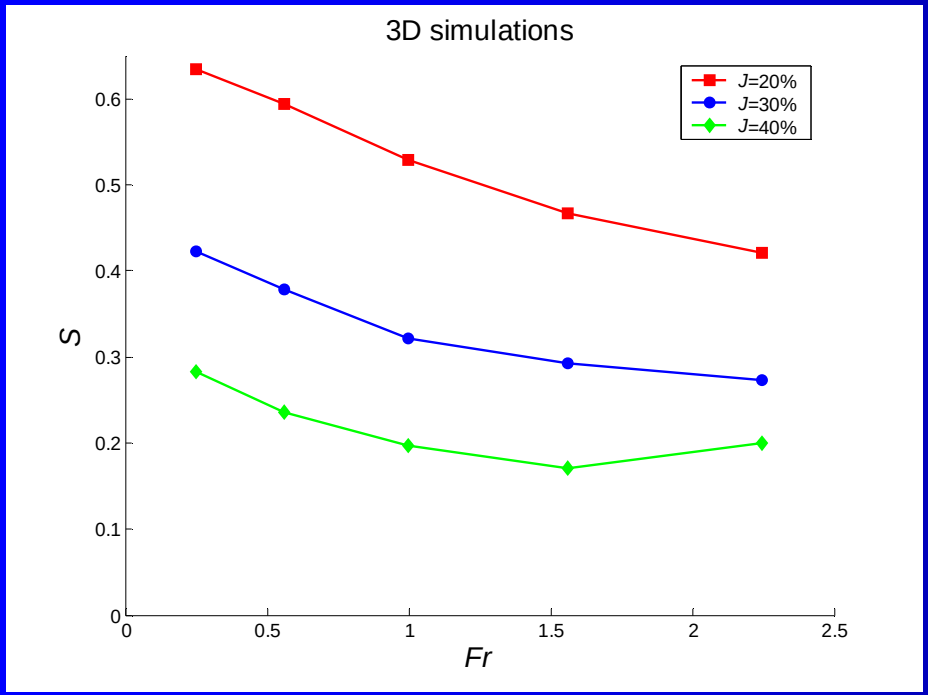

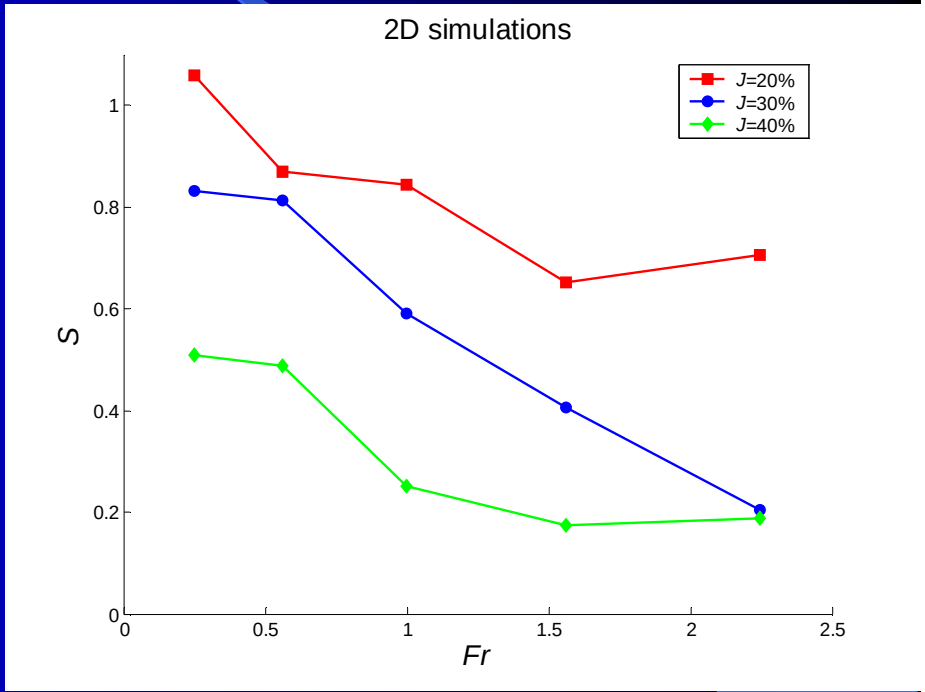

Faster transverse mixing in 2D than in 3D

Conclusions

- Longitudinal mixing
  - Diffusion equation
  - Diffusion coefficient
    - Proportional to rotational speed
    - Weak dependence filling degree
- Transverse mixing
  - Entropy-like mixing index
  - Mixing speed S
    - $\Omega \uparrow : S \downarrow$
    - $J \uparrow : S \downarrow$

Further research

- Effect of particle properties on mixing
- Non-spherical particles
- Inclined rotary kilns
- Velocity profile in active layer
- Inclusion of gas flow
- Axial segregation